**A NEW TAILORING OPTIMIZATION APPROACH FOR IMPROVING
STRUCTURAL RESPONSE AND ENERGY ABSORPTION
CAPABILITY OF LAMINATED AND SANDWICH COMPOSITES**

Ugo Icardi and Laura Ferrero

A NEW TAILORING OPTIMIZATION APPROACH FOR IMPROVING STRUCTURAL RESPONSE AND ENERGY ABSORPTION CAPABILITY OF LAMINATED AND SANDWICH COMPOSITES

UGO ICARDI AND LAURA FERRERO

This paper is dedicated to the memory of Liviu Librescu.

In this paper a technique for tuning the energy absorption properties of laminated and sandwich composites through a new tailoring concept is presented. The purpose is to minimize the energy absorbed through unwanted modes (ones involving interlaminar strengths) and maximize that absorbed through desired modes (ones involving membrane strengths) by finding a suited in-plane variable distribution of stiffness properties. Herein mode is intended as a strain energy contribution, such as bending energy, in-plane and out-of-plane shear energy, etc., and no vibration mode. This distribution is obtained making extremal certain strain energy contributions of interest (for example, membrane, bending, in-plane, and out-of-plane shear energies) under in-plane variation of the plate stiffness properties. The effect of this technique is to act as an energy absorption tuning, since it minimizes or maximizes the amount of energy absorbed by specific modes. Although the present technique could be applied to laminates or to the face sheets of sandwich composites, in this paper a preliminary application is presented to single plies with variable stiffness coefficients over their plane. Once incorporated into a laminate or a sandwich composite, these layers are shown to have beneficial effects on the strength at the onset of delamination in sample cases where laminated and sandwich composites are subjected to low velocity, low energy impacts.

1. Introduction

As is well known, fiber reinforced and sandwich composites with laminated faces offer advantages over conventional metallic structures in terms of specific strength and stiffness, impact resistance, containment of explosions, protection against fragments' projection, survivability, noise, and vibration suppression. Beside many other, not cited favorable properties, they also offer the remarkable advantage of being tailored to fulfill design requirements.

Unfortunately, these materials absorb a large amount of the incoming energy through local failures. The effect of this damage accumulation usually appears at the global level as an embedded delamination. A significant accumulation is detrimental, since it could degrade strength and stiffness, cause a deleterious load redistribution, and reduce the service life. Obviously, an accurate assessment of the local damage mechanisms and postfailure behavior is mandatory, in order to fully exploit the potential advantages of these materials. The reader is referred to the review papers [Rowlands 1985; Tennyson and Wharam 1985;

Nahas 1986; Bolotin 1996; Echaabi and Trochu 1996; Paris 2001; Icardi et al. 2007] for a comprehensive discussion of the local failure mechanisms and residual properties of these materials, these being outside the scope of this paper.

Various techniques have been recently published with the aim of preventing the damage accumulation, reducing its effects, and obtaining an improved structural performance. Functionally graded materials [Fuchiyama and Noda 1995] avoid unwise stress concentrations at interfacial material discontinuities that conventional fiber reinforced and sandwich composites exhibit, by virtue of the gradual variation of their physical properties. Technological skills such as stitching, lap and T joints, or short rods have been suggested in order to improve the transverse shear strength of multilayered materials and limit the detrimental effects of local damage and delamination propagation. These skills oppose cracks and sliding displacements by inducing bridging tractions, as shown by Cox [1999], although at the expense of the stress concentrations induced by the local tractions that oppose the propagation of the delamination. An improvement in the impact and delamination resistance and in dissipation can be achieved by stacking layers with different absorption and dissipation properties, namely, plies with customary properties and viscoelastic layers [Suzuky et al. 2003]. Since the viscoelastic layers must be as thick and numerous as the structural layers, this method unfortunately makes the structures too flexible and is not effective for sandwich composites, because the number of damping layers being incorporated is lower than in laminated composites. Moreover, the stresses in the adhesive film which bonds the viscoelastic layers to the host structure could limit the strength and the service life.

Several studies dealing with methods which seek to simultaneously improve stiffness, energy absorption, and dissipation have been recently published. Jung [2001] seeks to comply stiffness and energy dissipation by combining different materials with different absorption and stiffness properties. Lakes [2002] shows that the structural hierarchy makes it possible to obtain of both the desired stiffness and damping properties. McCoucheon [2004] shows that the energy dissipation can be increased without remarkable stiffness loss by inserting fluid filled microtubes into a matrix material, where the fluid flow is induced by the composite deformation. Actual tailoring, meaning the optimization of the reinforcement orientation and constituent materials, is preferred to these techniques because they introduce technological complications. Recently, variable stiffness composites in which the orientation of the fibers minimizes the stresses were studied, for example, by Pedersen [2003] and Setoodeh et al. [2005]. Other recent studies by Zinoviev and Ermakov [1994] and Georgi [1979] investigated the effects of the fibers" orientation (constant over the plate) for finding configurations able to dissipate a large amount of the incoming energy, while keeping the wanted strength and stiffness properties.

In the present paper a new approach based on a variable spatial distribution of stiffness properties is presented. Its aim is to limit the detrimental effects of damage and improve the structural performance of fiber reinforced and sandwich composites by optimizing the energy absorption properties. With this approach, contrasting objectives for currently available optimization techniques such as improvement of stiffness and, contemporaneously, of delamination strength, can be conjugated. The idea proposed is finding a variable spatial distribution that makes stationary the strain energy contributions as desired (for example, bending, in-plane, and out-of-plane modes), in order to allow a maximization of the energy stored in wanted modes (for example, in-plane modes and membrane strengths) and a minimization of that stored in unwanted modes (for example, out-of-plane shears, etc.). The appropriate in-plane distribution of plate stiffness coefficients is obtained making extremal the strain energy contributions of

interest under in-plane variation of the plate stiffness properties, and enforcing conditions which range from the imposition of the thermodynamic constraints, to the choice of a convex or a concave shape (in order to minimize or maximize the energy contributions of interest), to the imposition of a mean value for these coefficients. To account for these optimized stiffness variations either the fiber orientation, the constituent materials, the volumetric rate of fibers, or the thickness of plies could be varied.

In this paper, a preliminary application to single plies with optimized variable stiffness coefficients is presented, but the actual technique could be applied also to laminates or to the face sheets of sandwich composites as well, numerically solving the Euler–Lagrange equations. Two optimized ply stiffness distributions with complementary properties are proposed; they are based on an approximate parabolic solution of these equations. Their mean stiffness properties are chosen to be the same as that of the corresponding plies made of the same constituent materials having constant stiffness. The first type allows an increased bending stiffness, at the expense of a moderate increase of transverse shear stresses; the second type does just the opposite. In this way, the delamination damage could be increased and used to absorb the incoming energy. The replacement of a couple of conventional, constant stiffness layers in laminated and sandwich composites with these layers will appear able to consistently reduce the through the thickness interlaminar stress, either keeping the bending stiffness substantially unchanged or improving it, for all the sample cases considered in the numerical applications. In the case of low velocity, low energy impacts they will be shown to always produce beneficial effects on the strength at the onset of delamination for both laminated and sandwich composites with laminated faces.

The case of low velocity, low energy impacts was chosen because it is dominated by delamination and matrix cracking and is always responsible for a relevant strength degradation, even when the barely visible impact damage is not evident. There is a general agreement that for this kind of impact the energy is mainly absorbed as strain energy and through local failures, thus strain rate dependent formulations and microstructure level considerations are reputed as unnecessary; in addition, the deformation of the projectile is considered negligible [Davies and Olsson 2004]. Since the contact duration is higher then the stress waves' lateral transit time, transverse shear waves reflect off the edges several times while the contact load is still being applied, so the plate structural modeling, the plate size, and the boundary conditions affect the response. Stress based criteria are used to predict the onset of delamination, since it is a common opinion that they are accurate enough for this task. Three different delamination criteria, which appeared accurate in literature, are considered in order to have mutual assessments. The effects of the accumulated damage are accounted for, reducing the elastic properties of the layers that failed, within the framework of the ply-discount theory. As customary for low velocity impacts, the time history of the contact force is computed using modified versions of Hertz's contact law; the dynamic equations are integrated through Newmark's technique.

Since the numerical results show that the interlaminar stresses can be consistently reduced through a variable in-plane distribution of stiffness properties, keeping a high stiffness, future applications are expected where the local effects are accounted for in a much more detailed way. In subsequent sections the features of the models used will be briefly summarized, the energy storage optimization process discussed in detail, and the numerical applications presented.

2. Structural modeling

No attempt is made to review the ample literature about the modeling of laminated and sandwich composites. We refer to the available survey papers and monographs for a comprehensive discussion of this topic [Reddy 1982; 1990; 2003; Bert 1984; Librescu and Reddy 1986; Noor and Burton 1989; 1990; 1992; Noor et al. 1996; Reddy and Robbins 1994]. We just remind the reader that to accurately model the energy contributions involved, the layerwise kinematics and their inherent stress fields have to be accounted for as accurately as possible and, to limit the computational costs and storage, as efficiently as possible. To this purpose, in this paper a three-dimensional zigzag model [Icardi 1998; 2001], and the corresponding $C°$ eight node plate element [Icardi 2005; Icardi and Zardo 2005], both based on the five DOF of customary plate models, are employed as structural models. The three-dimensional zigzag model has the advantage of requiring a low computational effort, like conventional single layer plate models, with higher accuracy. This makes its use affordable within the optimization process for finding the stiffness distribution. The finite element is based on a conventional first order shear deformation plate element, to which a procedure for updating the strain energy to that of the three-dimensional zigzag model and a postprocessing technique based on a high order spline representation of the nodal DOF (which is used in place of the low order representation by shape function for obtaining integrated stresses) are applied, which makes the computation of interlaminar stresses accurate, but saves computational and memory storage costs. The mixed brick element with three displacements and three interlaminar stresses as nodal DOF developed by Icardi and Atzori [2004] is used to compute the local effects of the optimized solutions with the highest accuracy.

The capability of the present computational model to predict the local failures and the impact induced delamination damage has been successfully assessed in a number of previously published papers [Icardi and Zardo 2005; Icardi and Ferrero 2005; 2006a; 2006b; 2006c; 2007a; 2007b; Ferrero and Icardi 2006; 2007; Icardi 2007]. It appears from the comparison with ultrasonic inpsection detections of impact induced delamination damage and force time history detections that this simple modeling of the impact with a low computational effort is capable of accurate predictions of the delamination damage.

A variety of models, the so called layerwise models, have been developed. They have different features, degree of accuracy, and computational effort. In a broad outline, they subdivide into discrete layer and zigzag models, as aforementioned, if they impose the interfacial continuity requirements as constraint conditions, or if they postulate an appropriate piecewise variation of displacements, respectively. Both kinds of models are used in this paper, to exploit their complementary performance in terms of accuracy and computational effort. Their characteristic features are briefly summarized.

Perhaps the most general zigzag representation of displacements is the one developed by Icardi [2001] and subsequently improved in [Icardi 2007]. Unfortunately, this model is difficult to treat within the optimization process, since a big mathematical effort is required. For this reason, a third order zigzag model with a constant transverse displacement, which only accounts for the discrete layer effects of transverse shears, is particularized and used within the optimization process. In order to improve the accuracy of this model, its strain energy is updated to that of the previous model in the applications where the response of laminates incorporating optimized layers is studied using an approach based on the method of weighted residuals, instead of the finite element model described in the next section. This updating is carried out as outlined by Icardi [2005], using the postprocessing technique presented therein

to obtain a realistic prediction of interlaminar stresses. The mixed, eight node solid element used in this study was developed by Icardi and Atzori [2004]. It has the three interlaminar stresses and the three elastic displacements as nodal DOF, in order to fulfill the interfacial stress and displacement continuity requirements. Characteristic feature, C°, trilinear, and standard serendipity shape functions are used for interpolating the DOF across the element volume. In this way, the intraelement equilibria are met in an approximate integral form, according to Zienkiewicz and Taylor [1994]. As customary, the required level of variation of the layerwise quantities is obtained by increasing the number of subdivisions across the thickness. This makes the structural model computationally intensive, but accurate, as shown by Icardi and Atzori [2004]. The readers will find a compendium on hybrid and mixed (we reserve the term mixed for the case where the master fields are internal fields and the term hybrid for when surface fields are involved) finite elements for composites in the recent book by Hoa and Feng [1998], and the omitted details on development of the present element and an assessment of its accuracy in [Icardi and Atzori 2004].

Since displacements and stresses are interpolated with the same functions, the intraelement equilibrium conditions are met in an approximate integral form. This approach, seldom used, though efficient, makes easier the development of mixed elements and does not compromise the accuracy [Loubignac et al. 1978; Nakazawa 1984]. The generation of the stiffness matrix and the vector of nodal forces follows the standard path.

The representation of the chosen nodal DOF makes the computational effort required by the present element similar to that of displacement based counterpart solid elements, while accuracy and convergence are dramatically improved [Icardi and Atzori 2004]. Furthermore, it enables the element to be implemented into commercial finite element codes.

3. Optimization of the energy storage

As previously mentioned, the present paper aims to improve the structural performance of laminated and sandwich composites, optimizing the energy absorption properties of the constituent layers. The concept involved is finding optimized spatially variable stiffness properties which make stationary the bending, in-plane, and out-of-plane contributions to the strain energy, as desired. In this way, the energy absorbed by modes having detrimental effects (meaning, involving weak properties) is transferred to acceptable modes by minimizing the energy contributions involved in the unwanted modes (for example, transverse shears) and maximizing those of the acceptable ones (for example, membrane loading). As a result of this energy "tuning", stiffness and delamination strength, which are contrasting objectives for currently available constant stiffness optimization techniques, can both be improved.

The optimization of the energy storage starts writing the membrane, bending, in-plane, and out-of-plane strain energy contributions appearing in the zigzag model, for a generic laminate (herein sandwich composites are viewed as multilayered materials). Since standard variational calculus techniques are used, no details of these techniques are here discussed. It is just reminded that setting to zero the first variation of a functional coming from a weak form produces a set of governing equations, the so called Euler–Lagrange equations, that recover the strong forms of the weakened field equations and natural boundary conditions. In the present case, the stiffness properties will represent the master field, while the other variables not subjected to variation will represent the slave and data fields. Therefore, the
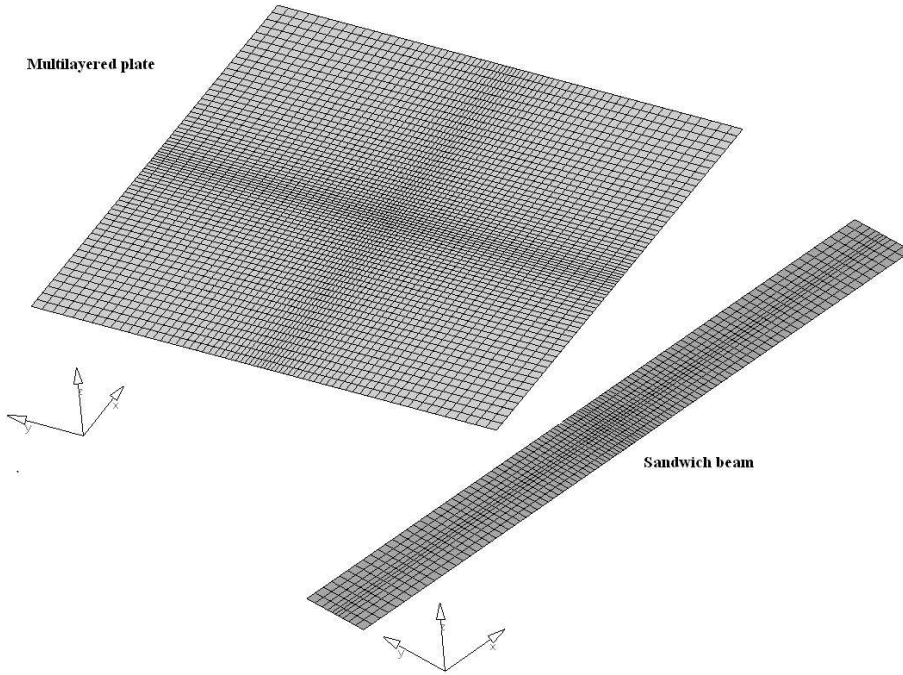
Figure 1. Discretizations used in the optimization process with the zig zag finite element. The multilayered plate is described in Section 4.2 and the sandwich beam analyzed in Section 4.4.

Euler–Lagrange equations will represent the relations enabling the stiffness properties to make the strain energy contributions extremal. The solution of these equations finds the stiffness distributions making minimal or maximal the desired energy contributions, meaning the in-plane variable distribution of the reinforcement fibers' orientation, the fiber volume rate, and the constituent materials.

3.1. *Stationary conditions for the strain energy contributions.* The basic step for the optimization of the energy absorption is to write the first variation of the strain energy for the zigzag model and to set it to zero, since it represents the equilibrium condition that the optimized solutions must fulfill. This variation is expressed in terms of stress resultants. The readers are referred to the paper by Icardi [1998] for the explicit expressions of the numerous and quite complex stress resultants in terms of the stiffness quantities of the zigzag model and of the continuity functions they involve.

According to the present paper's aim, assume the elastic stiffness coefficients Q_{ij} of each lamina to be functions of position in the lamina (x, y) plane. Since the three principal material directions can have a different orientation point to point, the thermodynamic constraints of Appendix A will need to be checked and, if necessary, enforced in a pointwise sense, as outlined subsequently. Assume the orthotropic relations hold locally at any point.

We list below the stationary conditions for each of the energy contributions of the zigzag model, obtained under variation of the stiffness properties of layers in the x and y directions. The conditions are expressed in terms of stiffness quantities and functional DOF derivatives, using the notation defined

in Appendix B. The equations can be applied irrespectively of the lay-up (that is, symmetric and non-symmetric can both be considered), since they are coupled by the large number of coupling stiffness coefficients appearing in Appendix B.

For notational convenience, we set $\eta = h^{-}1$.

(i) Stationary condition for the bending energy contribution:

$$-WR1\delta u^{(0)} - WR2\delta v^{(0)} - WR3\delta w^{(0)} + \left(WR4 - \tfrac{4}{3}WR5 + WR6 + WR7\right)\delta\gamma_x{}^{(0)}$$
$$+ \left(WR8 - \tfrac{4}{3}WR9 + WR10 + WR11\right)\delta\gamma_y{}^{(0)} = 0. \quad (1)$$

(ii) Stationary condition for the shear energy contribution in the (x, z) plane:

$$\left\{XR_{R1} + XR_{R1}^a + XR_{R1}^d + XR_{R44} + XR_{R44}^a + XR_{S44}^d - \tfrac{4}{3}\eta^2(XR_{P1} - XR_{P6})\right.$$
$$\left. -\tfrac{1}{2}\eta(XR_{26X2}+XR_{31X2}+XR_{36X2}+XR_{41X2})-\tfrac{2}{3}\eta^2(XR_{26X3}+XR_{31X3}+XR_{36X3}+XR_{41X3})\right\}\delta u^{(0)}$$
$$+\left\{XR_{R2} + XR_{R2}^a + XR_{R2}^d + XR_{R55} + XR_{R55}^a + XR_{S55}^d - \tfrac{4}{3}\eta^2(XR_{P2} - XR_{P7})\right.$$
$$\left. -\tfrac{1}{2}\eta(XR_{27X2}+XR_{32X2}+XR_{37X2}+XR_{41X2})-\tfrac{2}{3}\eta^2(XR_{27X3}+XR_{32X3} + XR_{37X3} + XR_{42X3})\right\}\delta v^{(0)}$$
$$+\left\{XR_{R3} + XR_{R3}^a + XR_{R3}^d + XR_{R66} + XR_{R66}^a + XR_{S66} + XR_{S66}^d - \tfrac{4}{3}\eta^2(XR_{P3} + XR_{P8})\right.$$
$$\left. -\tfrac{1}{2}\eta(XR_{28X2} + XR_{33X2} + XR_{38X2} + XR_{43X2}) - \tfrac{2}{3}\eta^2(XR_{28X3} + XR_{33X3} + XR_{38X3} + XR_{43X3})\right\}\delta w^{(0)}$$
$$+\left\{XR_{R4} + XR_{R4}^a + XR_{R4}^d + XR_{R88} + XR_{R88}^a + XR_{S88}^d - XR_{T88} - XR_{T88}^a - XR_{T88}^d\right.$$
$$-\tfrac{4}{3}\eta^2(XR_{P4} + XR_{P9}) + 4\eta^2 XR_{RR1} - \tfrac{1}{2}\eta(XR_{29X2} + XR_{34X2} + XR_{39X2} + XR_{44X2})$$
$$\left. -\tfrac{2}{3}\eta^2(XR_{29X3}+XR_{34X3}+XR_{39X3}+XR_{44X3})+\eta(XR_{46X1}+XR_{48X1})+2\eta^2(XR_{46X2}+XR_{48X2})\right\}\delta\gamma_x{}^{(0)}$$
$$+\left\{XR_{R5} + XR_{R5}^a + XR_{R5}^d + XR_{R99} + XR_{R99}^a + XR_{S99}^d - XR_{T99} - XR_{T99}^a - XR_{T99}^d\right.$$
$$-\tfrac{4}{3}\eta^2(XR_{P5} + XR_{P10}) + 4\eta^2 XR_{RR2} - \tfrac{1}{2}\eta(XR_{30X2} + XR_{35X2} + XR_{40X2} + XR_{45X2})$$
$$\left. -\tfrac{2}{3}\eta^2(XR_{30X3}+XR_{35X3}+XR_{40X3}+XR_{45X3})+\eta(XR_{47X1}+XR_{49X1})+2\eta^2(XR_{47X2}+XR_{49X2})\right\}\delta\gamma_y{}^{(0)}. \quad (2)$$

(iii) Stationary condition for the shear energy contribution in the (y, z) plane:

$$\left\{YR_{R1} + YR_{R1}^b + YR_{R1}^b + YR_{R44} + YR_{R44}^b + YR_{S44}^b - \tfrac{4}{3}\eta^2(YR_{P1} - YR_{P6})\right.$$
$$\left. -\tfrac{1}{2}\eta(YR_{26Y2} + YR_{31Y2} + YR_{36Y2} + YR_{41Y2}) - \tfrac{2}{3}\eta^2(YR_{26Y3} + YR_{31Y3} + YR_{36Y3} + YR_{41Y3})\right\}\delta u^{(0)}$$
$$+\left\{YR_{R2} + YR_{R2}^b + YR_{R2}^c + YR_{R55} + YR_{R55}^b + YR_{S55}^c - \tfrac{4}{3}\eta^2(YR_{P2} - YR_{P7})\right.$$
$$\left. -\tfrac{1}{2}\eta(YR_{27X2} + YR_{32X2} + YR_{37X2} + YR_{41X2}) - \tfrac{2}{3}\eta^2(YR_{27X3} + YR_{32X3} + YR_{37X3} + YR_{42X3})\right\}\delta v^{(0)}$$
$$+\left\{YR_{R3} + YR_{R3}^b + YR_{R3}^c + YR_{R66} + YR_{R66}^b + YR_{S66} + YR_{S66}^c - \tfrac{4}{3}\eta^2(YR_{P3} + YR_{P8})\right.$$
$$\left. -\tfrac{1}{2}\eta(YR_{28Y2} + YR_{33Y2} + YR_{38Y2} + YR_{43Y2}) - \tfrac{2}{3}\eta^2(YR_{28Y3} + YR_{33Y3} + YR_{38Y3} + YR_{43Y3})\right\}\delta w^{(0)}$$
$$+\left\{YR_{R4} + YR_{R4}^b + YR_{R4}^c + YR_{R88} + YR_{R88}^b + YR_{S88}^c - YR_{T88} - YR_{T88}^b - YR_{T88}^c - \tfrac{4}{3}\eta^2(YR_{P4} + YR_{P9})\right.$$
$$+4\eta^2 YR_{RR1} - \tfrac{1}{2}\eta(YR_{29Y2}+YR_{34Y2}+YR_{39Y2}+YR_{44Y2}) - \tfrac{2}{3}\eta^2(YR_{29Y3}+YR_{34Y3}+YR_{39Y3}+YR_{44Y3})$$
$$\left. +\eta(YR_{46Y1} + YR_{48Y1}) + 2\eta^2(YR_{46Y2} + YR_{48Y2})\right\}\delta\gamma_x{}^{(0)}$$
$$+\left\{YR_{R5} + YR_{R5}^b + YR_{R5}^c + YR_{R99} + YR_{R99}^b + YR_{R99}^c - YR_{T99} - YR_{T99}^b - YR_{T99}^c - \tfrac{4}{3}\eta^2(YR_{P5} + YR_{P10})\right.$$
$$+4\eta^2 YR_{RR2} - \tfrac{1}{2}\eta(YR_{30Y2} + YR_{35Y2} + YR_{40Y2}YR_{45Y2}) - \tfrac{2}{3}\eta^2(YR_{30Y3} + YR_{35Y3} + YR_{40Y3} + YR_{45Y3})$$
$$\left. +\eta(YR_{47Y1} + YR_{49Y1}) + 2\eta^2(YR_{47Y2} + YR_{49Y2})\right\}\delta\gamma_y{}^{(0)}. \quad (3)$$

The quantities XR_{ijX3}, YR_{ijY3} (for $i=2$ and $j=6, 7, 8, 9$; $i=3$ and $j=0$ to 9; $i=4$ and $j=0$ to 9), which are not defined in Appendix B, are obtained in a straightforward way changing Equation (2) with Equation (3) into the definitions therein reported for XR_{ijX2} and YR_{ijY2}.

Homogenizing the virtual variations, so as to convert the derivatives of virtual displacements, the Euler–Lagrange equations making extremal each of the desired strain energy contributions are obtained in the form of partial differential equations in terms of plate stiffness quantities of the laminate.

These extremal equations have to be elaborated in order to collect all the contributions that multiply a specific virtual displacement, since it is arbitrary inside the domain. As a result a rather intricate system of coupled, partial differential equations in terms of the laminate stiffness quantities is obtained.

For practical reasons, since the displacements, the number of layers in the laminate, and the constituent materials are arbitrary, as a preliminary application the optimization procedure is next applied to a single constituent lamina of a laminated or sandwich composite. The problem turns into an extremal problem at the ply level where we try to find optimized plies which, once incorporated in place of preexisting layers, can improve the structural performance of laminated and sandwich composites, whatever the lay-up, boundary conditions, and loading might be.

In the next part of this section, the stiffness distributions which make extremal the bending and shear energy contributions of a single ply will be searched.

3.2. *Optimized single ply.* An approximate solution, of technical interest, to the resulting set of partial differential equations (1)–(3) for a single constituent ply is the following second order polynomial approximation for the transformed reduced stiffness coefficients,

$$Q_{11} = A_1 + A_2 x + A_3 x^2, \tag{4}$$

$$Q_{22} = B_1 + B_2 y + B_3 y^2, \tag{5}$$

$$Q_{12} = C_1 + C_2 x + C_3 y + C_4 x^2 + C_5 y^2 + C_6 xy, \tag{6}$$

$$Q_{66} = D_1 + D_2 x + D_3 y + D_4 x^2 + D_5 y^2 + D_6 xy, \tag{7}$$

$$Q_{16} = E_1 + E_2 x + E_3 x^2 + E_4 xy, \tag{8}$$

$$Q_{26} = F_1 + F_2 y + F_3 y^2 + F_4 xy, \tag{9}$$

$$Q_{44} = G, \tag{10}$$

$$Q_{55} = L, \tag{11}$$

$$Q_{45} = M, \tag{12}$$

where A_1, $A_2, \ldots$, $B_1, \ldots$, F_1, G, L, and M are coefficients to be determined by enforcing desired conditions. Although many other conditions could be enforced, those arising from the imposition of means stiffness properties are considered in this paper. In consequence of their enforcement, the mean stiffness of optimized layers is made equal to that of the customary layers they replace. In this way, the comparison between the lay-up with optimized layers and the conventional ones can be carried out keeping the average properties unchanged. In addition, the thermodynamic constraints listed in Appendix A have to be enforced, in order to make the optimized ply a real material [Jones 1999]. Finally, convexity or concavity have to be chosen, in order to minimize or maximize the energy contributions whose variation is set to zero. Note that Equations (4), (5), and (8)–(12) provide an exact solution and identically fulfill

the thermodynamic constraints, while (6) and (7) are approximate and require these constraints to be enforced. The formulas (6) and (7) exactly fulfill the extremal conditions in the equations where only second order derivatives of the stiffness coefficients appear. However almost all the terms involving third and higher order derivatives vanish for an insulated lamina. As a consequence, the present solution is a suboptimal approximation; it is motivated by the need to find a solution of technical interest, compatible with the current technologies.

In Section 4, the performance of laminates incorporating few layers that minimize the bending strain energy and maximize the transverse shear energy, or vice versa, will be assessed. Since the features of the solution could depend on the model used, the set of governing equations being different from one structural model to another, the performance of the present approximation will be tested using the mixed solid element of Section 2 and, in a few cases, the zigzag plate model and the related energy updating, within the framework of Galerkin's approach. The basic features concerning the modeling of the contact force used in the impact studies of Section 4 will be summarized.

3.3. *Modeling of the impulsive loads.* The impact problems can be classified according to the impactor velocity (or energy) as a low velocity, an intermediate, a ballistic, or a hyper velocity impact [Davies and Olsson 2004]. A different modeling has to be used in each of these cases.

Although the velocities and the energies indicated as threshold in literature can vary consistently, the researchers agree that for low velocity impacts, the object of this paper, since they are always responsible for a relevant strength degradation even when the so called barely visible impact damage is not evident, the incoming energy is mainly absorbed as strain energy and through local failures. This kind of impact is dominated by delamination and matrix cracking, rather than by penetration induced fiber breakage like in the other cases [Joshi and Sun 1987].

Since the contact duration is higher then the stress waves' lateral transit time, transverse shear waves reflect off the edges several times while the contact load is still being applied. Due to this, the accuracy of the structural modeling, the plate size, and the boundary conditions strongly affect the response. On the contrary, strain rate effects are marginal due to the low speed, so the material properties can be assumed unchanged from the static ones in the low velocity impacts. Although more sophisticated approaches could be used where the impactor and the structure are discretized by three-dimensional finite elements, the contact force can also be successfully simulated simply using modified versions of the Hertzian contact law, provided that the involved parameters are appropriately set either by numerical and analytical techniques, or by experiments. This is what appears in a large number of studies published in the literature [Tan and Sun 1985; Wu and Shyu 1993; Matemilola and Stronge 1995; Yigit and Christoforou 1995; Carvalho and Guedes Soares 1996; Lee et al. 1997; Liou 1997; Choi 2006]. The Hertzian contact law correlates the contact force $\mathscr{F}$ with the indentation depth α, by a parameter called the contact stiffness K_c. The contact region is required to be small, while the vibration of the striking mass and the frictional forces must be negligible. The problem can be divided into three phases: loading, unloading, and reloading. In the present paper, in the loading phase we use the relation $\mathscr{F}(t) = \mathscr{K}_c \alpha(t)^{3/2}$. The exponent $3/2$ was chosen because it appears in very good correlation with a great amount of experimental tests published in the literature for carbon, Kevlar, glass reinforced, and sandwich composites (see the aforementioned relevant samples), while K_c needs to be estimated for each case (the target and the projectile materials, etc.). Various techniques for evaluating K_c have been proposed, which are either based on analytical

	E_{11}	E_{22} (E_{33})	G_{12}	G_{13}	G_{23}	ν_{12} (ν_{23})	Density
Faces	142	9.8	7.1	7.1	3.3	0.3 (0.5)	1617.3
Cores		(0.138)		0.041	0.024	0.5 (0.02)	48

Table 1. Material properties of the sandwich panel, with units of GPa, except for ν, unitless, and density, in kg/m^3.

and numerical approaches or on direct derivation from laboratory tests. With the advent of recent three-dimensional nonlinear finite elements able to accurately simulate the contact problem, the available commercial finite element codes can be conveniently used to determine the relation between force and indentation depth. In the present paper, the finite element code Mecalog Radioss was used for this purpose; the constituent layers were discretized by a three-dimensional meshing, where the fibers and matrix were described by solid elements. As the loading phase ends, a significant permanent indentation takes place even when the composites are relatively thin. In this phase the relative motion between the target structure and projectile changes sign, thus a new law has to be used; in the present paper, we apply the formula, first suggested by Crook [1952], $\mathscr{F}(t) = \mathscr{F}_m \left((\alpha - \alpha_0) / (\alpha_m - \alpha_0) \right)^q$. $\mathscr{F}_m$ is the load at which the unload phase starts, α_m is the relative indentation depth, both easily determined from the loading phase curve, while α_0 is the permanent indentation depth, which in the present paper has been estimated by Mecalog Radioss. The exponent q is set to 2.5, because this value fits the experiments presented in the literature for a variety of laminated and sandwich composites. This unloading curve has to be used every time the contact force decreases; moreover, in the event of bounces, a reloading law is also required.

The indentation used in the reloading phase formula is the difference between the permanent and the current one. Because the properties are degraded after the first loading phase, the transverse material properties, and consequently the contact rigidity, change; this is indicated by $\mathscr{K}_c\prime$. We use the reloading law $\mathscr{F}(t) = \mathscr{K}_c\prime \, (\alpha - \alpha_0)^p$, with the exponent p set to 1.5, according to experiments. The contact force computed as outlined above is transformed into an equivalent force distributed at the nodes in the finite element discretization.

This simplified approach for modeling the contact force was chosen because it provides results always in a good agreement with the experiments in the case of low velocity impacts, as shown by many researchers [Tan and Sun 1985; Wu and Shyu 1993; Matemilola and Stronge 1995; Yigit and Christoforou 1995; Carvalho and Guedes Soares 1996; Lee et al. 1997; Liou 1997; Choi 2006; Icardi and Zardo 2005; Icardi and Ferrero 2005; 2006a; 2006b; 2006c; 2007a; 2007b; Ferrero and Icardi 2006; 2007; Icardi 2007], and is easy to implement.

The Newmark implicit time integration scheme is used for solving the contact problem, because the explicit time integration schemes need extremely small time steps to be stable. The reader is referred to Icardi and Zardo [2005] for details about this method.

In the former applications [Icardi and Ferrero 2005; 2006a; 2006; 2006b; 2006c; 2007a; 2007b; Ferrero and Icardi 2007; Icardi 2007] this impact model always provided a contact force time history in good agreement with the experiments, and, where available, with the damage detected via ultrasonic inspection. As a further assessment, in this paper the impact problem on a sandwich plate is considered.

The sample case here examined was formerly investigated by Choi [2006], who assessed the accuracy of the spring element method, with or without considering von Karman nonlinear strains, since locally deformations can be rather large. The material properties for this sample case are reported in Table 1. The sandwich panel has sides of 102×102, the constituent layers have a thickness of 0.175 mm, the face sheets have a $[0°/90°]$ lay-up, the core is 25.4 mm thick, and all the edges are fixed. It is impacted by a 1.61 kg steel sphere with a velocity of 1.2 m/s. The contact force time history obtained by the present model is reported in Figure 2, where it is compared with that of Choi [2006]. The results from the present model have been obtained either using linear or nonlinear strain displacement relations of the von Karman type, and two structural models, the present zigzag model and the FSDPT model. It appears the accuracy of the zigzag model improved and the effects of nonlinearity on it were negligible. In contrast, the accuracy of the simplified structural model by Choi [2006] is consistently improved using nonlinear strains. Since nonlinearity was shown to have a mild effect on the zigzag model, the next results will refer to linear strains. Many results are available in the literature which confirm that a linear approach is also quite accurate for sandwich composites, because they have a relevant crushing at the impact point only if the face sheets are very thin. Checks made using the model of Goldberg [2001] have shown the strain rate effects to be negligible, due to the low velocity and energy involved in all the sample cases considered; thus these effects will not be accounted for in the next section.

4. Numerical applications

The technique for tuning the energy absorption mechanism previously illustrated is now applied to several sample cases of practical interest. The aim is to assess whether it enables a simultaneous improvement
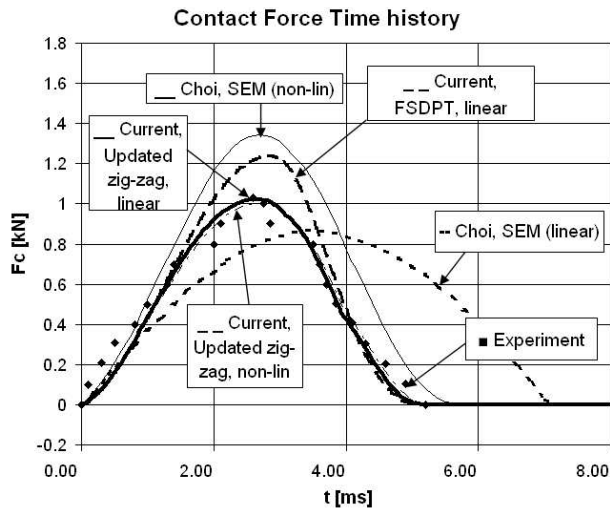

Figure 2. Contact force time history for a sandwich plate. Comparison between experimental test and some numerical results, obtained with five different techniques: the spring element method, linear and nonlinear, by Choi [2006], the current procedure with low refined structural model (FSDPT) and refined model (zigzag), in linear and nonlinear formulation.

of strength, stiffness and delamination resistance pursuing a magnitude reduction of interlaminar shear stresses, which are partly converted into membrane stresses. So, an advantage of the current technique is to operate on quantities (such as the interlaminar stresses) which affect the delamination strength without reducing beneficial properties such as the stiffness, as occurs with the currently available techniques for improving the delamination strength through use of viscoelastic layers, since they can make too deformable the laminates where they are incorporated. In this technique, the bending, shear, and membrane stiffness coefficients are locally changed, keeping the global stiffness unchanged. In other words, since the current stress based criteria consider the interlaminar stresses of primary importance for delamination, the current energy tuning technique works on these stresses. Whether it can reduce them and whether this fact has beneficial effects over the failure index, it can be intended as a technique for improving delamination. Future studies have to be carried out using much more sophisticated delamination models in order to understand the role played by damping and to better describe the damage process. Since the present technique seems to have relevant advantages, the use of much more accurate, but also computationally more intensive, models seems justified. It is however expected that the current technique will not considerably change the damping, because the variation of the fiber orientation involved occurs in a range where experimental results in the literature show mild variations of damping, and because these variations interest a couple, or very few, layers in a laminate. The loadings of interest here are impact loadings because they cause a variety of local failures and large delaminated zones across the thickness.

The present technique is illustrated through the following specific samples:

- Before applying them to the cases of interest, preliminary tests are presented in the Section 4.1 to assess the present technique and to illustrate its capability. A comparison is presented between a simply supported panel in cylindrical bending, made with a classical metallic material, and its carbon fiber, epoxy resin optimized counterpart. The aim is to limit deflections, although the mean bending stiffness is the same in the two cases.

- In Section 4.2 multilayered, simply supported plates undergoing impact loads are compared. Displacements and stresses of a lay-up with customary constant stiffness constituent layers are compared with those of counterpart plates in which two layers with optimized features and the same mean stiffness of the layers they substitute are incorporated at various positions across the thickness.

- In Section 4.3 a parametric study is reported in order to show the beneficial effects of the optimized lay-ups for some advantageous solutions to the aforementioned problems.

- In Section 4.4 the optimized layers are incorporated in the faces of a multicore sandwich beam in several positions, in order to further test the effectiveness of the present technique. The sandwich beam has two external faces and an internal one, splitting the core in two parts. It is subjected to an impulsive load and its performances are compared to those obtainable with classical layers, in terms of transverse stress field and local failure index.

4.1. *Single layer panel.* Consider a simply supported, metallic plate in cylindrical bending under a uniformly distributed transverse loading, which will enable us to draw observations of general validity. Let the goal be to minimize the deflection by an optimized composite layer with the same mean properties of the metallic beam. Assume these to correspond to an Al7075 alloy (see Table 2). The equilibrium

Type of material	Application	E_L (GPa)	E_T (GPa)	G_{LT} (GPa)	ν_{LT}
AL7075 alloy	Isotropic plate	71.00	26.69	0.33	
Carbon-HM	Fibers constituent (1)	380.00	NA	NA	0.69
Carbon-A	Fibers constituent (2)	210.00	NA	NA	0.69
Kevlar149	Fibers constituent (3)	130.00	NA	NA	0.30
Epoxy resin	Matrix constituent (1)	5.00	5.00	1.85	0.35
Polyethylene	Matrix constituent (2)	0.05	0.05	0.02	0.30
Carbon-epoxy (1)	Composite ply	138.00	138.00	5.99	0.28
Carbon-epoxy (2)	Composite ply	205.00	50.00	82.00	0.25

Table 2. Materials used in the numerical applications of Section 4.

equations are solved using Gelerkin's method and the updating process. The solution that minimizes bending is

$$D_{11} = 6.35 \times 10^2 + 2.0 \times 10^2 \frac{x}{L} - 2.0 \times 10^2 \left(\frac{x}{L}\right)^2. \tag{13}$$

The higher order stiffness contribution F_{11} is treated in the same way. The terms D_{22}, D_{12}, D_{16}, D_{26}, D_{66}, F_{12}, etc., are not involved in this problem since a cylindrical deformation is considered. An application to a plate under bidirectional sinusoidal loading which considers these contributions will be presented later. Consider various length to thickness ratios to have an indication of the gain obtainable, defined as the ratio gain $= (w_{\max} - w_{\max}^{\text{opt}})/(w_{\max})$, $w_{\max}$ being the maximum, or central, deflection of the metallic plate and $w_{\max}^{\text{opt}}$ that of the optimized composite plate. Choose a ratio between the minimum (at the bound) and the maximum (at the center) bending stiffnesses close to zero. The result obtained is that the gain increases till it reaches an asymptote, observed at about $L/h = 100$, corresponding to a gain of 18%, which shows that the optimization is always effective in the range of thickness variation of technical interest. The optimized stiffness distribution of Equation (13) could be obtained by varying the thickness of the lamina, or, more interestingly by the practical point of view, by varying the fibers and matrix constituent materials, their relative volume fraction, or varying point by point the orientation of fibers. If the fiber volume fraction is varied, while all the other parameters remain unchanged, the optimal stiffness distribution is obtained as

$$V_{\text{fibers}} = \left[\frac{h^3}{2.20 \times 10^1 + 4.8 \times 10^4 \, x/L - 4.8 \times 10^4 \, (x/L)^2} \frac{1}{1 - \nu^2} - \frac{1}{E_m}\right] \left(\frac{1}{E_f} - \frac{1}{E_m}\right),$$

according to the mixture rule, where V_{fibers} is the volumetric rate of the fibers, while E_m and E_f are the elastic moduli of the matrix and of the fibers. According to previous considerations, an optimized distribution of stiffness is conveniently obtained using low cost fibers, but a high quality matrix.

Figure 3 shows an assessment of a suboptimal, step distribution of different materials. This simple option appears of technical interest since it decreases deflection by 40%. Furthermore, the results of an analysis by the mixed solid element, not reported here for brevity, show that the local effects at the transition points are mild, although E_{11} of the fibers steeply changes from 40 to 517 GPa. This result shows that the use of high quality materials is effective at the center of plates, while at the bounds low quality materials can be used.
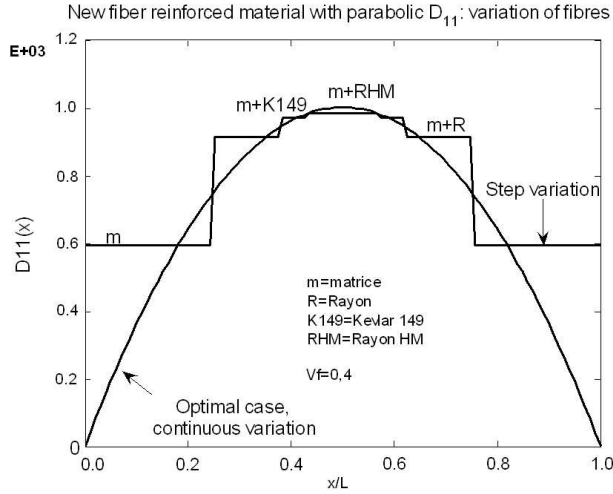
New fiber reinforced material with parabolic D_{11}: variation of fibres

Figure 3. Optimized and step variation of bending stiffness, as obtained by varying the reinforcement fibers.

Here no chemical compatibility considerations are discussed; they are left to a future study. Finally, the optimal orientation θ of the reinforcement fibers, keeping unchanged the other material parameters, is represented in Figure 4. It features a variation from $0°$ to $24°$, thus compatible with braiding and filament winding techniques. It can be smoothed at the bound with no remarkable performance loss (less than 3%), as numerically assessed.

4.2. *Impacted multilayered plate.* Consider a panel of length 10 cm, width 5 cm, and thickness 1 cm, with a $\left[45°/-45°/0_2°/45°/-45°\right]_s$ symmetric and balanced lay-up, which is simply supported at the bounds and subjected to a center point impact. For this panel, the contact force time history measured
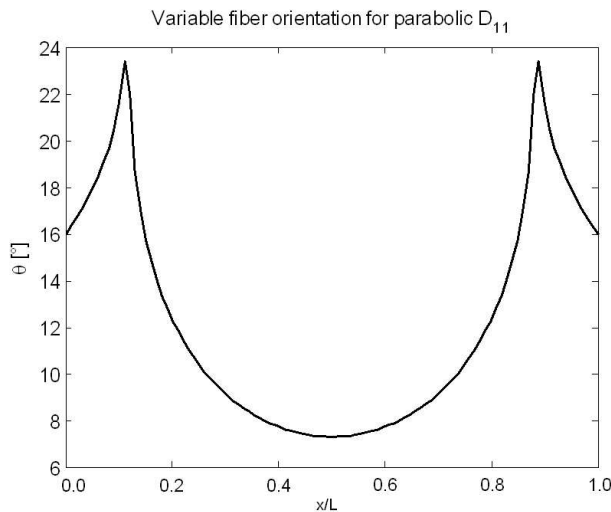
Variable fiber orientation for parabolic D_{11}

Figure 4. Variable reinforcement fiber orientation for minimizing bending.

Panel	E_{11}	E_{22}	G_{12}	G_{13}	G_{23}	ν_{12}	Density
	130	8	5	5	2.5	0.3	1557
Impactor		Nose diameter	Mass	Impact energy	E	ν	
		25.4	5.451	40	210	0.3	

Table 3. Material properties of the laminated panel and impactor characteristics, with E and G in GPa, ν dimensionless, density in kg/m^3, nose diameter in mm, mass in kg, and impact energy in J.

during an experiment is reported in the papers by Icardi [2005] and Icardi and Zardo [2005], to which the readers are referred for the details here omitted. Being rather thick, this panel has interlaminar stresses nearly of the same magnitude of the membrane stresses, so it is suited for applying the present tailoring optimization. The material properties, the impact energy, and the impactor characteristics are reported in Table 3, while the material strengths are reported in Table 4. The FE discretization is depicted in Figure 1. This sample has to be ascribed to the class of low velocity impacts, for which the strain rate effects

	X_t	Y_t	Z_t	X_c	Y_c	Z_c	S_{12}	$S_{13}-S_{23}$	S_i
A	0.167	0.06	0.101	0.108	0.17	0.23	0.07	0.0700–0.069	0.069
B	0.210	0.074	0.074	0.11	0.18	0.24	0.086	0.0860–0.064	0.064
C	0.009	0.009	0.0014			0.022		0.0086–0.0064	0.064

Table 4. In plane and out-of-plane material strengths, in GPa, for the laminated and sandwich panels. Row A is the strengths of the laminated panel, row B those of the sandwich panel faces, and row C those of the sandwich panel cores (foam).

Lam 0	Lam A	Lam B	Lam C	Lam D	Lam E	Lam F	Lam G	Lam H
45	a	a	c	c	45	45	45	a
-45	c	a	a	c	-45	-45	-45	-45
0	0	0	0	0	a	a	0	b
0	0	0	0	0	c	a	0	0
45	45	45	45	45	45	45	a	45
-45	-45	-45	-45	-45	-45	-45	a	a
-45	-45	-45	-45	-45	-45	-45	a	a
45	45	45	45	45	45	45	a	45
0	0	0	0	0	c	a	0	0
0	0	0	0	0	a	a	0	b
-45	c	a	a	c	-45	-45	-45	-45
45	a	a	c	c	45	45	45	a

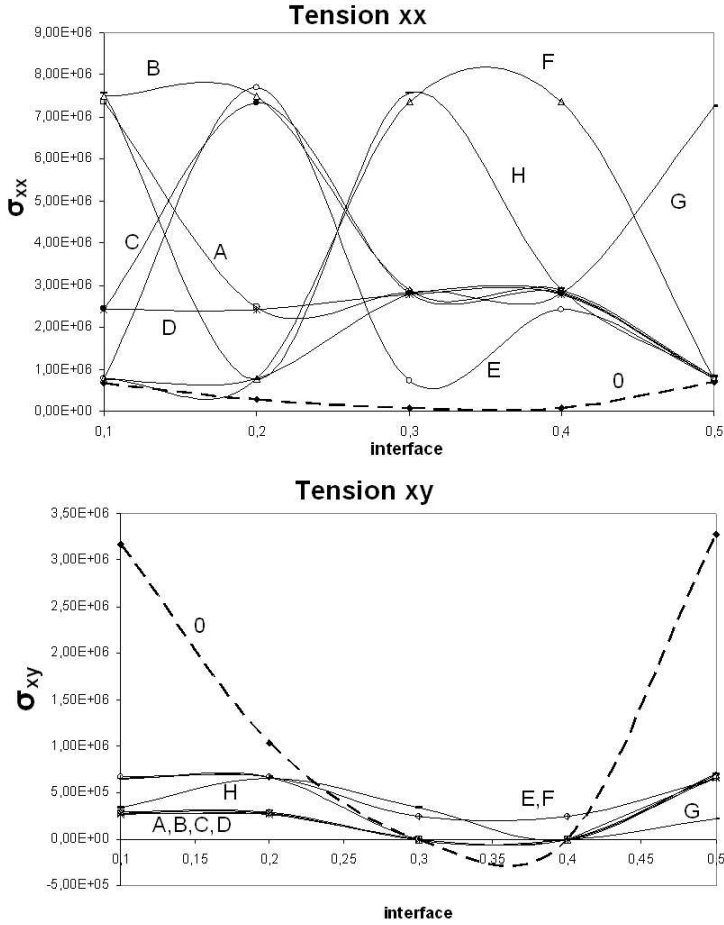**Table 5.** Stack-ups considered in the problem of Figure 8.

Figure 5. Panels subjected to an impact force: lay-ups considered, membrane stress, and in-plane shear stress. The dashed line shows unoptimized lay-up.

are negligible, as universally agreed by the most representative authors in the field. To assess whether the use of optimized layers can beneficially modify unwise stress fields, we will compare its structural performance with those of plates obtained substituting a couple of layers with optimized layers, in various positions across the thickness. The contact force is recomputed for these stack-ups using the approach outlined above. Consider three kinds of optimized layers:

 (i) A layer that minimizes bending and maximizes membrane energy,

 (ii) A layer that minimizes bending and maximizes transverse shear,

(iii) A layer that maximizes bending and minimizes transverse shear.

In any case, the mean stiffness properties are maintained equal to those of the preexisting layers that are replaced with these optimized layers.

Type (a) is obtainable with the optimization technique shown in Section 3.1, acting on bending and membrane energy first variations so that an energy transfer takes place from the bending mode (the

unwanted one) to the membrane mode (the preferred one). Types (b) and (c) have been formulated with the same technique, but the energy contributions involved are now the bending and the transverse shear modes. In the first case the energy is transferred form bending to shear, while in the second case the transfer takes place in the opposite direction. The choice of these layers has specific reasons, which we will explain subsequently, since each optimized layer has some beneficial effects on the panel performances, depending on the type and the position in the stack-up.

Now consider the effects on the impact behavior of substituting the preexisting layers in the $[45°/-45°/0°_2/45°/-45°]_s$ laminate with optimized layers (types (a) and (c)). Incorporate symmetric layers of the previously described types across the thickness of the laminate, according to the scheme of Table 5. In this first example, the transfer from shear to membrane energy should be underlined, so the graphs shown in Figure 5 concern membrane stresses (they are just plotted in the x direction) and in-plane shear. The dashed line represents the unoptimized panel (for example, Lam 0), while a label describes which laminate has been considered (for example, from Lam A to Lam G); the stresses have been calculated at each internal interface, at the impact point. Every optimized laminate shows an higher membrane stress field, but a lower in-plane shear field, especially at the most critical interface, the outer internal one. Similar observations can be drawn for the y direction.

Now consider a plate with the same dimensions of the previous one and the lay-up $[0°/45°/90°/-45°/0°]_s$. Consider in this case layers (a), (b), and (c) one type at a time, and incorporate them according to the scheme presented in Table 6. Figure 6 shows four plots pertaining to the center deflection, the transverse normal stress across the thickness, and the transverse shear stresses σ_{xz} and σ_{yz} in the spanwise direction, respectively, when the two outer plies are substituted with minimum bending layers of type (a). In this case, the effect of incorporating optimized layers is to strongly reduce deflections and interlaminar shears. In addition, it increases the membrane stresses (which help to suppress the damage spreading, like in pressurized structures) and the in-plane shear, but these results are here omitted for length, since their variations are not remarkable.

Basic	Var1a	1b	1c	Var2a	2b	2c	Var3a	3b	3c	Var4a	4b	4c	Var5a	5b	5c
0°	Type a	b	c												
45°				Type a	b	c									
90°							Type a	b	c						
-45°										Type a	b	c			
0°													Type a	b	c
0°													Type a	b	c
-45°										Type a	b	c			
90°							Type a	b	c						
45°				Type a	b	c									
0°	Type a	b	c												

Table 6. Stack-ups considered for the impact problem. Blank cases represent unchanged data with respect to the basic case with constant stiffness properties. Optimized layers are: type (a) with minimum bending and maximum membrane; type (b) with minimum bending and maximum shear; and type (c) with maximum bending and minimum shear.
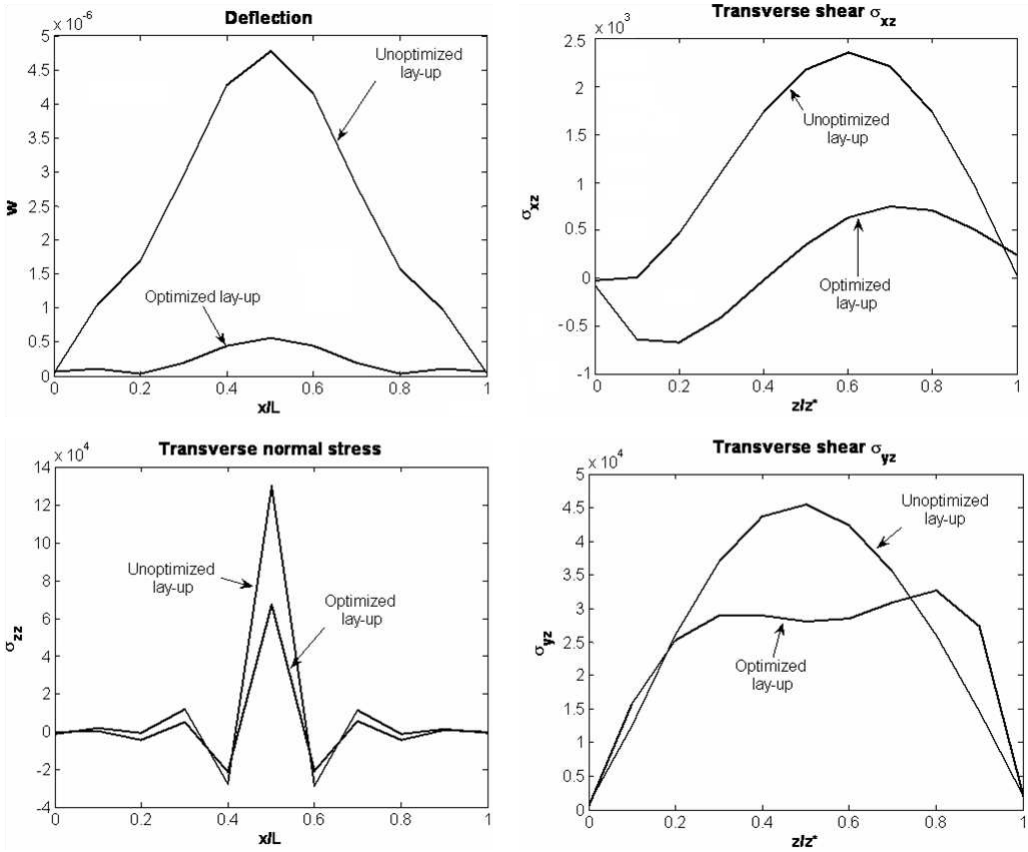
Figure 6. Deflection, transverse normal stress, and shear in the spanwise direction, and transverse shear across the thickness when the two outer plies are substituted with two minimum bending plies (type (a)). Comparison with the unoptimized lay-up.

The impact induced damage for this panel is computed at each interface nearby the impact point using three different stress based delamination criteria: the Hou, Petrinic, Ruiz, and Hallet criteria [Hou et al. 2000; 2001]; the Choi–Chang criteria [Choi and Chang 1992]; and the Chai–Gädke criteria [Chai and Gädke 1999]. These criteria have been chosen because they have found a number of successful applications in the literature to solution of this problem, and because they are easy to implement into finite element codes. To be concise, the failure index formulae are not reported. They can be found in [Icardi et al. 2007], to which the readers are referred also for a discussion of available delamination criteria. It is reminded that the stress based criteria are held by the leading scientists in this field to be accurate enough for predicting the delamination onset, but not the delamination growth. In the latter case, accurate results can be obtained only using fracture mechanics or progressive delamination models. The Choi–Chang criterion, which makes use of in situ properties, appears to be the most accurate criterion in all the published applications. Thus it will be used in all the numerical applications of this paper. In this section, the criterion of [Hou et al. 2000; 2001] will be also used, while in Section 4.4, the criterion of Chai–Gädke, which also makes use of in situ properties, is used. These additional criteria are considered

in order to see whether the proposed technique is effective, irrespective of the criteria used, and whether there can be a relevant variation of the strength at the onset of delamination using different criteria.

The strength at the onset of delamination of the basic panel with constant stiffness layers is compared to fifteen variations of it, which are obtained by replacing the preexisting layers with optimized layers, according to the scheme reported in Table 6 (for example, var1a, var1b, ..., var5a, ..., var5c, and layers (a), (b), and (c)). Table 7 reports the results by the Choi–Chang criterion, while Figure 7 presents those by the Hou, Petrinic, Ruiz, and Hallet criteria. It appears by these results that the effects on the impact induced delamination are beneficial across the thickness of embodying the optimized layers. It appears that the majority of the solutions embodying optimized panels bring significant improvement in the impact resistance with respect to the classical lay-up. It appears that improvements are obtained especially at the most critical interfaces.

4.3. *Parametric study for the laminated plate.*

Finally, a parametric study about the effects of variation of thickness and stack-up is presented. This analysis is aimed at defining what thickness range allows the best exploitation of the optimized layers and which position in the stacking sequence grants more evident effects. Let first focus on the thickness. Figures 8 and 9 report the results pertaining a variation of the overall thickness from 0.5 to 2 cm, with the width fixed at a value of 20 cm. In Figure 8 the deflection in the unoptimized plate and in the optimized plate var1a (refer to Table 6) are compared; the effects of the optimization is more evident for thin structures, but it is always effective for the deflection control. Figure 9 shows the transverse normal stress in the unoptimized plate and in the plate *var1b*; it appears that the beneficial effects of optimized plies are evident in the central region, while near the edges the tensional field is approximately unchanged for thick samples; on the contrary, the thin plates show lower
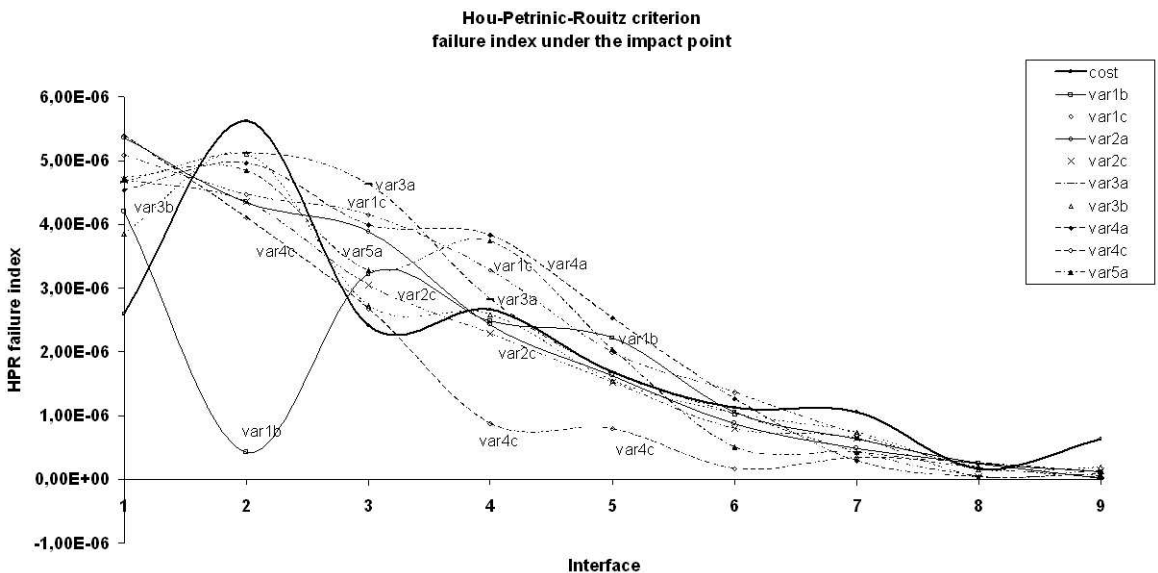

Figure 7. Failure index (dimensionless) according to the Hou–Petrinic–Ruiz criterion, at each interface, for the unoptimized lay-up (thick line) and for its variants, as defined in Table 7 (only the improved cases are reported).

Case	1	2	3	4	5	6	7	8	9
Basic	1.10E-08	5.56E-08	1.22E-07	2.18E-07	2.62E-07	2.44E-07	2.15E-07	1.41E-07	4.92E-08
var1a	3.93E-08	1.15E-07	1.07E-07	1.23E-07	1.25E-07	1.09E-07	1.05E-07	8.87E-08	5.49E-08
var1b	1.80E-08	7.42E-08	1.25E-07	1.98E-07	2.32E-07	2.14E-07	1.92E-07	1.37E-07	6.06E-08
var1c	4.95E-09	7.17E-09	1.29E-07	3.48E-07	4.38E-07	4.12E-07	3.63E-07	1.62E-07	4.65E-98
var2a	1.07E-09	5.41E-08	1.71E-07	1.90E-07	1.94E-07	1.73E-07	1.63E-07	1.40E-07	3.91E-08
var2b	7.45E-09	5.52E-08	1.34E-07	2.16E-07	2.44E-07	2.23E-07	1.95E-07	1.24E-07	4.13E-08
var2c	4.84E-08	1.18E-07	1.36E-07	2.14E-07	2.22E-07	1.95E-07	1.41E-07	5.55E-08	1.55E-08
var3a	6.80E-09	1.26E-08	9.37E-08	2.80E-07	2.92E-07	2.69E-07	2.57E-07	1.02E-07	9.27E-09
var3b	1.38E-08	6.57E-08	1.22E-07	1.99E-07	2.36E-07	2.16E-07	1.85E-07	1.24E-07	4.53E-08
var3c	9.36E-08	3.58E-07	3.85E-07	2.73E-07	1.67E-07	8.55E-08	3.64E-08	1.86E-08	7.54E-09
var4a	4.68E-09	1.46E-08	2.07E-08	2.38E-07	6.20E-07	5.96E-07	2.48E-07	4.21E-08	1.69E-08
var4b	1.03E-08	5.47E-08	1.31E-07	2.22E-07	2.52E-07	2.47E-07	2.09E-07	1.31E-07	4.66E-08
var4c	1.12E-07	5.33E-07	6.27E-07	3.87E-07	2.02E-07	4.47E-08	1.34E-08	1.90E-09	4.65E-09
var5a	7.10E-09	3.09E-08	5.93E-08	1.15E-07	4.97E-07	4.77E-07	1.20E-07	8.61E-08	3.32E-08
var5b	1.01E-08	5.38E-08	1.19E-07	2.17E-07	2.67E-07	2.46E-07	2.13E-07	1.43E-07	5.02E-08
var5c	1.37E-07	7.59E-07	9.53E-07	4.81E-07	1.13E-07	1.20E-07	2.76E-08	3.80E-08	5.18E-08

Table 7. Effects of optimized layer incorporation on delamination, according to the Choi–Chang criterion. Failure index (dimensionless) computed at each interface (the cases in the table) at the impact point for the basic panel with $[0°/45°/90°/-45°/0°]_s$ lay-up and fifteen variants embodying optimized layers.
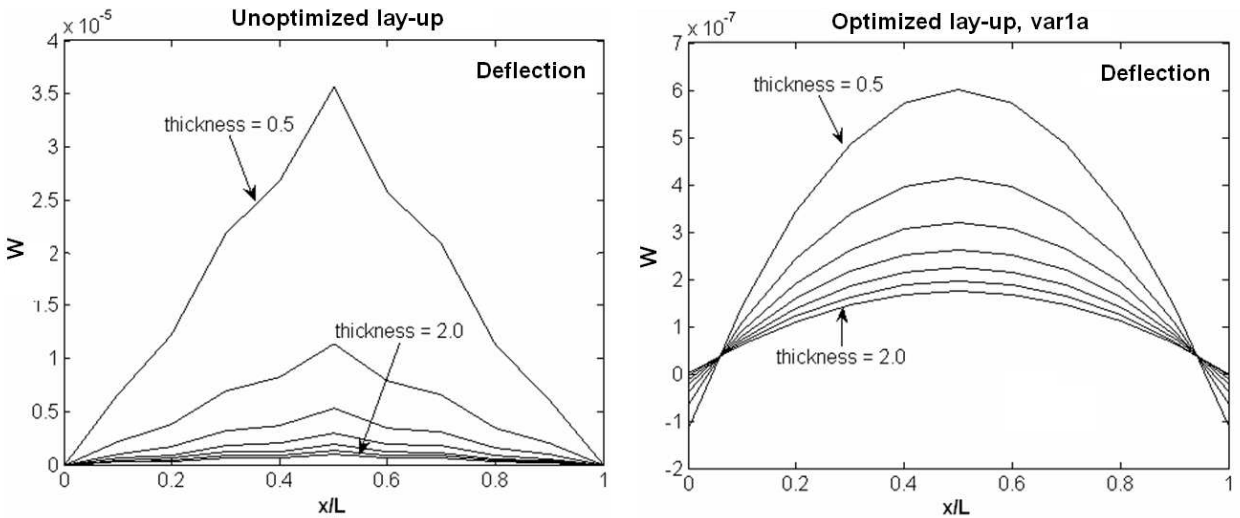

Figure 8. Deflection in the unoptimized plate and in the optimized plate (var1a), with increasing the total thickness.
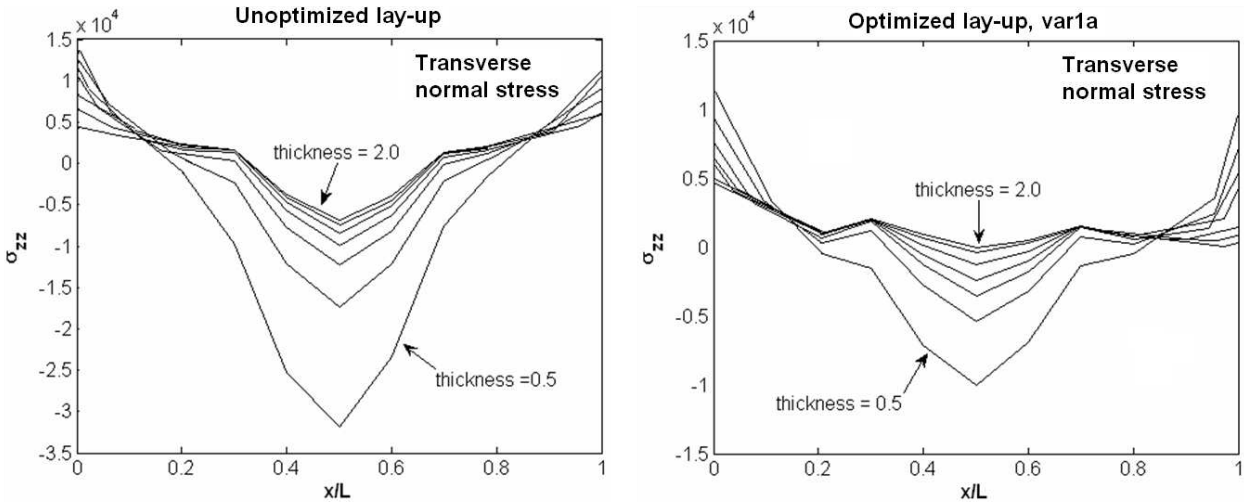
Figure 9. Transverse normal stress in the unoptimized plate and in the optimized plate (*var1b*) with increasing the total thickness.

tensional field also in the edges. Since the central region is the most damaged part, it can be guessed that the optimized (type (b)) layers are able to cut down the transverse normal stress.

Some considerations are now made about the influence of the stack-up. An extensive study has been performed in order to estimate the coupling effects, and it is possible to state that optimized structures show a good behavior even in nonsymmetric stack-ups. Moreover symmetric stack-ups are able to fulfill alternatively one of the two discussed aims, either the deflection control or the impact resistance improvement, with high gain compared to the classical plate. For this purpose, in Figure 10 four cases
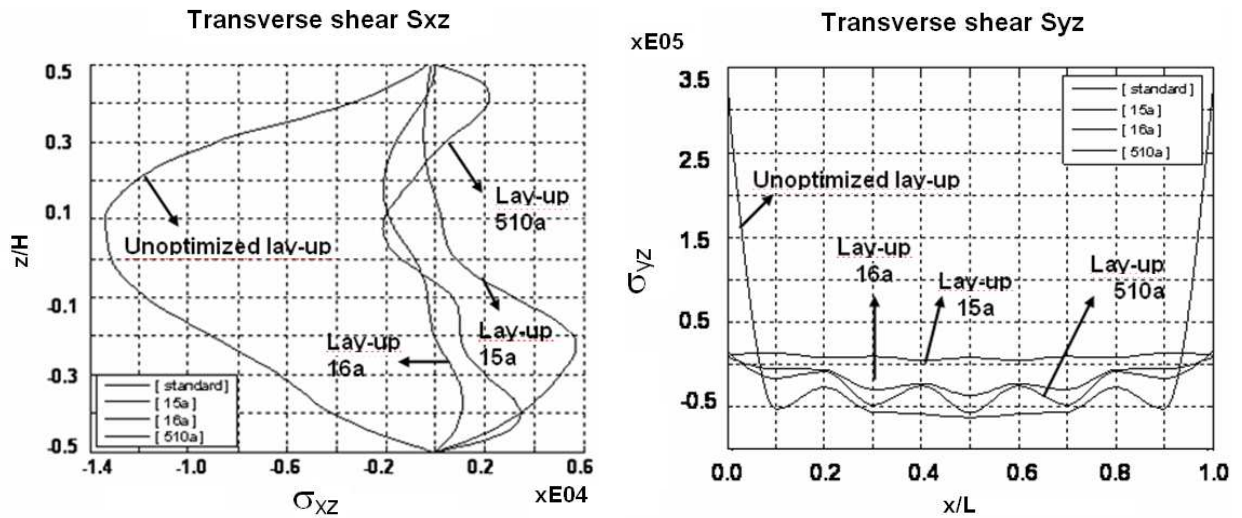

Figure 10. Transverse shear stress across the thickness and in the spanwise direction for the unoptimized plate and for three nonsymmetric optimized lay-ups.

are explored. The unoptimized plate, previously studied, is now subjected to a patch load in the four central nodes; starting from this basic stack-up, minimum shear plies have been introduced in positions 1 and 5, 1 and 6, and 5 and 10, in nonsymmetric lay-ups. In the transverse shears plotted against both directions, the classical plate develops the worst stress field. Meanwhile asymmetric stack-ups allow us to fulfill both the requirements, deflection reduction and impact resistance improvement, with quite good improvement compared to the unoptimized plates performances, but lower than what is obtainable with symmetric ones. In particular, across the thickness the optimized panels develop a lower shear field in the central region, where the unoptimized one reaches its maximum. Similarly, if the transverse shear is observed in the spanwise direction, at the most critical interface, the beneficial effects of the current technique is particularly clear near the edges, where the classical plate has a stress concentration. However, the most important result underlined in the present section is the good behavior of the optimized layers also when they are introduced in nonsymmetric positions, thanks to their capability to decouple bending and shear deformations.

4.4. *Impacted sandwich beam.*

The optimization process was above applied to laminates in order to assess the advantages in terms of impact strength, deflection, and interlaminar stress distributions. Now the optimization process is be applied to sandwich composites with laminated faces, which exhibit a critical impact behavior due to their high thickness and to the deep heterogeneity of their constituent materials. The aim of this section is to investigate the potential improvement of sandwich structures' critical behavior due to the introduction of the optimized plies. The sample here considered is a multicore sandwich structure made of two external faces, an internal one, and two cores (mechanical properties given in Table 1), which is clamped at the edges and impacted at the center with a steel sphere with a mass of 1.61 kg at speed 1.2 m/s. A 20×1 cm sandwich beam made up of 4 ply external faces, a 2 ply internal face, and two cores is considered. Every ply is 0.025 cm thick, while the cores are 0.5 cm thick, thus the overall thickness is 1.3 cm. Stack-up and geometry are described in Figure 11. The FE discretization is reported in Figure 1. Since this sample is still referring to a low velocity impact, again the strain rate effects are negligible. The optimized plies incorporated are minimum shear layers with properties which vary in the spanwise direction according to the law of Figure 12, where also the ratio between optimized and mean stiffnesses is plotted. As a first step, the transverse deflection is assessed, since it could have potential beneficial effects on the noise and vibration behavior. As shown in Figure 13, the transverse deflection can be radically cut off when optimized minimum shear layers replace classical plies, with a maximum gain of 35% when all the $0°$ plies are substituted. In addition, the interlaminar stresses should be monitored, in order to define whether the optimization is effective for enhancing the impact strength of sandwich plates. Looking at Figure 14, the transverse shear stress under the impact point can be compared among the three analyzed beams; it can be reckoned a strong reduction in the transverse shear, especially at the most critical interfaces, while the transverse normal stress is slightly increased, as shown in Figure 15. The transverse shear field appears to be lowered by the optimized ply introduction, since these plies appear able to minimize the energy stored in the shear mode and of maximize the bending and membrane mode. This action can be seen as an energy transfer from the unwanted out-of-plane modes to the membrane mode, as already occurred for the sample case of Section 4.2. Finally, the impact induced damage is estimated by computing stress based failure indexes close to the impact point. For this sample case the criteria of Choi–Chang, already used in Section 4.2, and those
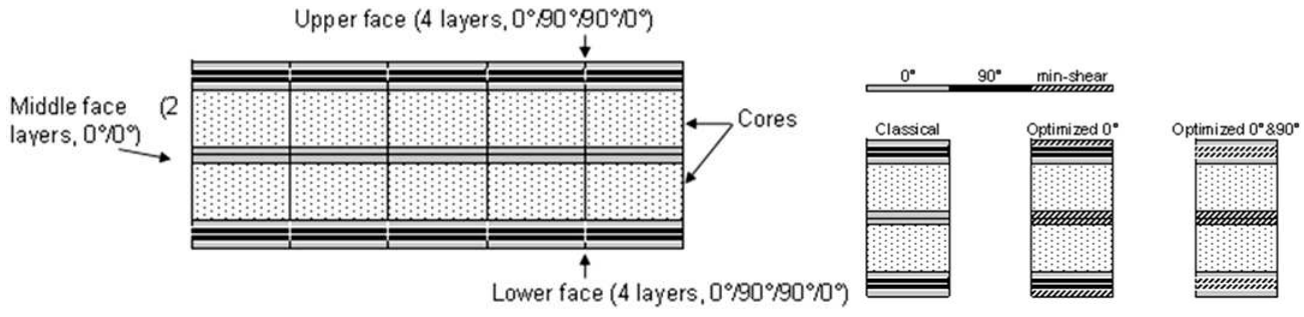
Figure 11. Geometry and stack-up of the dual-core sandwich beam; classical case with constant stiffness plies, optimized cases with minimum shear plies introduced in place of classical ones.
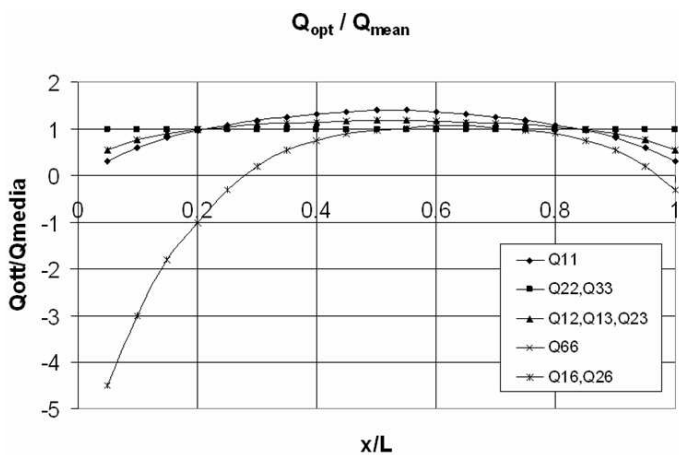

Figure 12. Stiffness law of variation in the spanwise direction for the minimum shear optimized layers.
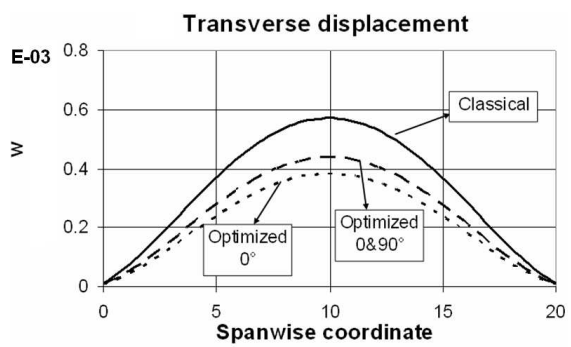

Figure 13. Transverse deflection of the dual core sandwich beam, in the classical configuration and in the optimized ones, obtained with minimum shear layers.
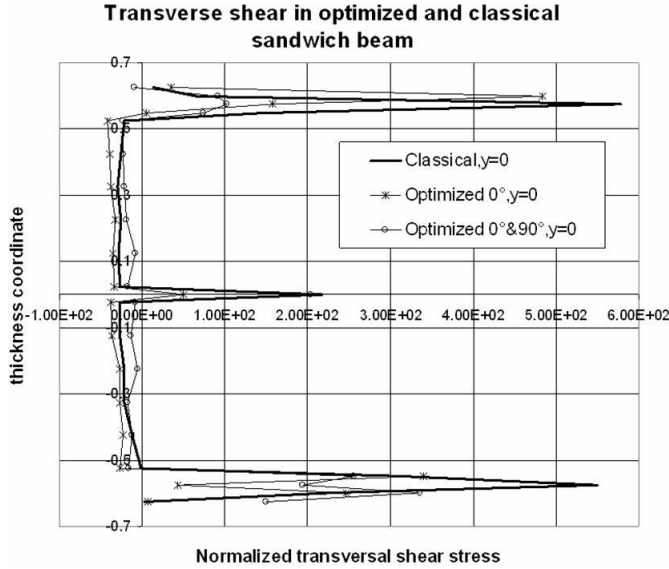
Figure 14. Transverse shear stress across the interfaces under the impact point; results for dual core sandwich beam, in the classical configuration and in the optimized ones, obtained with minimum shear layers.

of Chai–Gädke are considered, which are both based on in situ properties (see [Icardi et al. 2007] for a discussion and the explicit expressions of these criteria). In Figure 16, the damage computed by the above mentioned criteria is reported across the various interfaces under the impact point for the three analyzed structures. Comparing these cases, the effectiveness of the optimized layers can be assessed. It appears that a failure index reduction of 50% in the internal face and of 70% in the external ones can be obtained incorporating the optimized layers. Since the most critical aspect of sandwich structures is the damage arising at the core face interfaces, we can guess by these results that the current optimization technique has a beneficial effect in this region through a strain energy manipulation that reduces the transverse shears.

5. Concluding remarks

A theoretical study dealing with a technique for tuning the energy absorbed by laminated and sandwich composites with laminated faces in the bending, in-plane, and out-of-plane shear modes has been presented. The basic idea is to minimize the energy absorbed through unwanted modes (those involving interlaminar strengths) and maximize that absorbed through desired modes (those involving membrane strengths), by finding a suitable in-plane variable distribution of stiffness properties. This optimal distribution is found making the energy contributions of interest extremal under the properties' spatial variation. Therefore this new tailoring concept requires either the orientation of the reinforcement fibers, the constituent materials, or the fiber volume fraction to be varied. In this way, the incoming energy can be transferred among the modes which are made extremal, obtaining an increase or a decrease, as desired, of the single contributions with respect to the case of customary constant stiffness constituent plies,
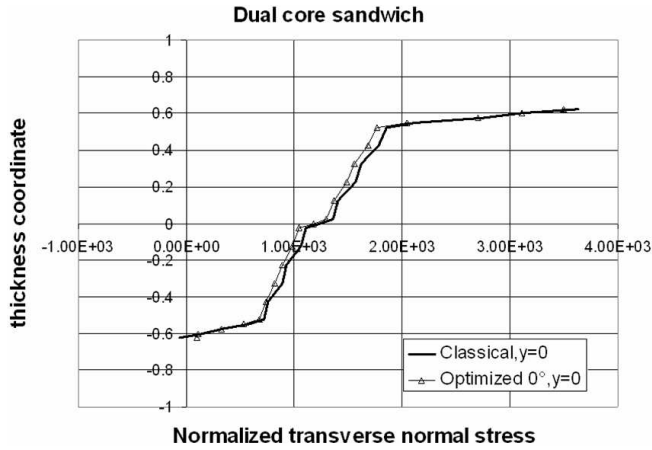
Figure 15. Transverse normal stress across the interfaces under the impact point; results for dual core sandwich beam, in the classical configuration and in the optimized ones, obtained with minimum shear layers.

assuming the mean stiffness properties of variable stiffness layers coincide with those of these layers. As a result, one can obtain an energy transfer from bending to in-plane and out-of-plane shear energy modes,
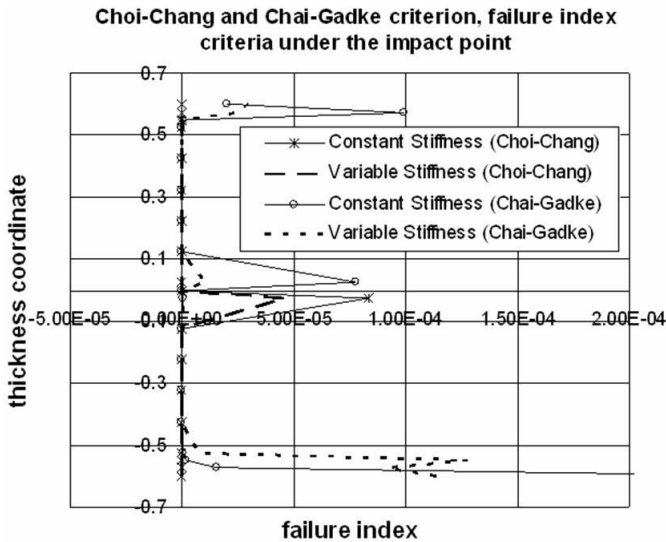

Figure 16. Failure index computed across the interfaces under the impact point; two stress based criteria have been used, Choi–Chang and Chai–Gädke, both involving in situ properties. Comparison between the optimized beam (with locally variable stiffness) and the classical one, with constant stiffness.

or vice versa, with respect to layers with customary properties. The optimized stiffness distribution is obtained enforcing conditions which range from the imposition of thermodynamic constraints to the choice of a convex or a concave shape (in order to minimize or maximize the energy contributions of interest), to the imposition of their mean value. The present technique has its main advantage in the possibility of conjugating reduced interlaminar stresses with a high stiffness, that is precluded to the currently available methods based on interposition of compliant layers. Two structural models with complementary features are used: a zigzag model, which is inexpensive but accurate, is used in the optimization process, while a mixed, eight node solid element is used to accurately assess the local effects of the optimized solutions. A preliminary application to single plies with variable stiffness coefficients is presented. Two types are considered: the first is a layer that strongly reduces bending without increasing the shear stresses, and the second is a layer which strongly reduces shear stresses without increasing deflections. Both can be obtained by current manufacturing technologies, a smooth variation of the reinforcement fibers orientation being required over their plane. The numerical applications presented concern laminated and sandwich composites subjected to low velocity impacts. These layers appear able to consistently reduce the through the thickness interlaminar stress concentrations and to keep the bending stiffness substantially unchanged, when appropriately positioned across the thickness. These preliminary results encourage future developments of the present technique.

Appendix A: Thermodynamic constraints

The stiffness coefficients are subjected to the thermodynamic constraints conditions hereafter reported (see, Jones (1999) for details). To fulfill conservation of energy, the stiffness $[Q_{ij}]$ and compliance $[Q_{ij}^{-1}]$ matrices must be positive definite. Thereby E_L, E_T, G_{LT} and G_{TT} must be positive. Likewise, the following condition by Lempriere:

$$\left[1 - v_{32}^2 \left(\frac{E_2}{E_3}\right)\right]\left[1 - v_{13}^2 \left(\frac{E_3}{E_1}\right)\right] - \left[v_{21} \left(\frac{E_1}{E_2}\right)^{1/2} + v_{13} v_{32} \left(\frac{E_2}{E_1}\right)^{1/2}\right]^2 > 0$$

must be fulfilled. The compliance coefficients S_{ij} also must fulfill following relations by Lekhnitski:

$$S_{66} = \frac{1}{G_{12}} \; ; \quad S_{16} = \frac{\eta_{12,1}}{E_1} = \frac{\eta_{1,12}}{G_{12}} \; ; \quad S_{26} = \frac{\eta_{12,2}}{E_2} = \frac{\eta_{2,12}}{G_{12}}$$

where

$$\eta_{i,ij} = \frac{\epsilon_{ii}}{\epsilon_{ij}} \; ; \quad \eta_{ij,i} = \frac{\epsilon_{ij}}{\epsilon_{ii}}$$

while the transverse shears must fulfill following relations in terms of Chentsov's coefficients $\eta_{ij,kl} = \epsilon_{ij}/\epsilon_{kl}$:

$$\frac{\eta_{ij,kl}}{G_{kl}} = \frac{\eta_{kl,ij}}{G_{ij}}$$

Appendix B: Stiffness derivatives

Recall that η is defined as h^{-1}.

$$WR1 = B_{11,111} + B_{12,122} + 3B_{16,112} + B_{26,222} + 2B_{66,122}$$

$$WR2 = B_{12,112} + B_{16,111} + 3B_{26,112} + B_{22,222} + 2B_{66,112}$$

$$WR3 = D_{11,1111} + 2D_{12,1122} + 4D_{16,1112} + 4D_{26,1222} + 4D_{66,1122} + D_{22,2222}$$

$$WR4 = D_{11,111} + D_{12,122} + 3D_{16,112} + D_{26,222} + 2D_{66,122}$$

$$WR5 = (F_{11}\eta^2)_{,111} + (F_{12}\eta^2)_{,122} + 3(F_{16}\eta^2)_{,112} + (F_{26}\eta^2)_{,222} + 2(F_{66}\eta^2)_{,221}$$

$$WR6 = D^a_{11,111} + D^a_{12,122} + 3D^a_{16,112} + D^a_{26,222} + 2D^a_{66,122}$$

$$WR7 = D^a_{12,112} + D^a_{22,222} + 3D^a_{26,122} + D^a_{16,111} + 2D^a_{66,112}$$

$$WR8 = D_{16,111} + 3D_{26,122} + 2D_{66,112} + D_{12,112} + D_{22,222}$$

$$WR9 = (F_{16}\eta^2)_{,111} + 3(F_{26}\eta^2)_{,122} + 2(F_{66}\eta^2)_{,112} + (F_{12}\eta^2)_{,112} + (F_{22}\eta^2)_{,222}$$

$$WR10 = D^b_{16,111} + 3D^b_{26,122} + 2D^b_{66,112} + D^b_{12,112} + D^b_{22,222}$$

$$WR11 = D^c_{11,111} + D^c_{12,122} + 3D^c_{16,112} + D^c_{26,222} + 2D^c_{66,122}$$

Define the following quantities for the shear energy contribution in the plane (x, z):

$$XR_{R1} = B_{11,11} + B_{16,12} \; ; \quad XR_{R2} = B_{16,11} + B_{12,12}$$

$$XR_{R3} = D_{11,111} + 2D_{16,112} + D_{12,122}$$

$$XR_{R4} = R_{1X,11} + R_{2X,12} \; ; \quad XR_{R5} = R_{3X,11} + R_{4X,12}$$

$$R_{1X} = D_{11} + D^a_{11} + D^d_{16} - \tfrac{4}{3}\eta^2 F_{11} \; ; \quad R_{2X} = D_{16} + D^a_{16} + D^d_{12} - \tfrac{4}{3}\eta^2 F_{16}$$

$$R_{3X} = D_{16} + D^b_{16} + D^c_{11} - \tfrac{4}{3}\eta^2 F_{16} \; ; \quad R_{4X} = D_{12} + D^b_{12} + D^c_{16} - \tfrac{4}{3}\eta^2 F_{12}$$

$$XR^a_{R1} = B^a_{11,11} + B^a_{16,12} \; ; \quad XR^a_{R2} = B^a_{16,11} + B^a_{12,12}$$

$$XR^a_{R3} = D^a_{11,111} + 2D^a_{16,112} + D^a_{12,122}$$

$$XR^a_{R4} = R^a_{1X,11} + R^a_{2X,12} \; ; \quad XR^a_{R5} = R^a_{3X,11} + R^a_{4X,12}$$

$$R^a_{1X} = D^a_{11} + D^{aa}_{11} + D^{ad}_{16} - \tfrac{4}{3}\eta^2 F^a_{11} \; ; \quad R^a_{2X} = D^a_{16} + D^{aa}_{16} + D^{ad}_{12} - \tfrac{4}{3}\eta^2 F^a_{16}$$

$$R^a_{3X} = D^a_{16} + D^{ab}_{16} + D^{ac}_{11} - \tfrac{4}{3}\eta^2 F^a_{16} \; ; \quad R^a_{4X} = D^a_{12} + D^{ab}_{12} + D^{ac}_{16} - \tfrac{4}{3}\eta^2 F^a_{12}$$

$$XR^d_{R1} = B^d_{16,11} + B^d_{66,12} \; ; \quad XR^d_{R2} = B^d_{66,11} + B^d_{26,12}$$

$$XR^d_{R3} = D^d_{16,111} + 2D^d_{66,112} + D^d_{12,122}$$

$$XR^d_{R4} = R^d_{1X,11} + R^d_{2X,12} \; ; \quad XR^d_{R5} = R^d_{3X,11} + R^d_{4X,12}$$

$$R^d_{1X} = D^d_{16} + D^{ad}_{16} + D^{dd}_{66} - \tfrac{4}{3}\eta^2 F^d_{11} \; ; \quad R^d_{2X} = D^d_{66} + D^{dd}_{66} + D^{dd}_{26} - \tfrac{4}{3}\eta^2 F^d_{66}$$

$$R^d_{3X} = D^d_{66} + D^{bd}_{66} + D^{ad}_{16} - \tfrac{4}{3}\eta^2 F^d_{16} \; ; \quad R^d_{4X} = D^d_{26} + D^{bd}_{26} + D^{cd}_{66} - \tfrac{4}{3}\eta^2 F^d_{26}$$

$$XR_{R44} = B_{16,12} + B_{66,22} \; ; \quad XR_{R55} = B_{66,12} + B_{26,22}$$

$$XR_{R66} = D_{16,112} + 2D_{66,122} + D_{26,222}$$

$$XR_{R88} = R_{9X,12} + R_{10X,22} \; ; \quad XR_{R99} = R_{11X,12} + R_{12X,22}$$

$$R_{9X} = D_{16} + D_{16}^a + D_{66}^d - \tfrac{4}{3}\eta^2 F_{16} \; ; \quad R_{10X} = D_{66} + D_{26}^a + D_{26}^d - \tfrac{4}{3}\eta^2 F_{66}$$

$$R_{11X} = D_{66} + D_{66}^b + D_{16}^c - \tfrac{4}{3}\eta^2 F_{66} \; ; \quad R_{12X} = D_{26} + D_{26}^b + D_{66}^c - \tfrac{4}{3}\eta^2 F_{26}$$

$$XR_{R44}^a = B_{16,12}^a + B_{66,22}^a \; ; \quad XR_{R55}^a = B_{66,12}^a + B_{26,22}^a$$

$$XR_{R66}^a = D_{16,112}^a + 2D_{66,122}^a + D_{26,222}^a$$

$$XR_{R88}^a = R_{9X,12}^a + R_{10X,22}^a \; ; \quad XR_{R99}^a = R_{11X,12}^a + R_{12X,22}^a$$

$$R_{9X}^a = D_{16}^a + D_{16}^{aa} + D_{66}^{ad} - \tfrac{4}{3}\eta^2 F_{16}^a \; ; \quad R_{10X}^a = D_{66}^a + D_{26}^{aa} + D_{26}^{ad} - \tfrac{4}{3}\eta^2 F_{66}^a$$

$$R_{11X}^a = D_{66}^a + D_{66}^{ab} + D_{16}^{ac} - \tfrac{4}{3}\eta^2 F_{66}^a \; ; \quad R_{12X}^a = D_{26}^a + D_{26}^{ab} + D_{66}^{ac} - \tfrac{4}{3}\eta^2 F_{26}^a$$

$$XR_{S44}^d = B_{12,12}^d + B_{26,22}^d \; ; \quad XR_{S55}^d = B_{26,12}^d + B_{22,22}^d$$

$$XR_{S66}^d = D_{11,112}^d + 2D_{66,122}^d + D_{22,222}^d$$

$$XR_{S88}^d = R_{13X,12}^d + R_{14X,22}^a \; ; \quad XR_{S99}^d = R_{15X,12}^d + R_{16X,22}^d$$

$$R_{13X}^d = D_{12}^d + D_{12}^{ad} + D_{26}^{dd} - \tfrac{4}{3}\eta^2 F_{16}^a \; ; \quad R_{14X}^d = D_{26}^d + D_{26}^{ad} + D_{22}^{dd} - \tfrac{4}{3}\eta^2 F_{66}^a$$

$$R_{15X}^d = D_{26}^d + D_{26}^{bd} + D_{12}^{cd} - \tfrac{4}{3}\eta^2 F_{66}^a \; ; \quad R_{16X}^d = D_{26}^d + D_{22}^{bd} + D_{66}^{cd} - \tfrac{4}{3}\eta^2 F_{22}^d$$

$$XR_{T88} = A_{44} - 4\eta^2 D_{44} + A_{44}^a + A_{45}^d \; ; \quad XR_{T99} = A_{45} - 4\eta^2 D_{45} + A_{44}^c + A_{45}^b$$

$$XR_{T88}^a = A_{44}^a - 4\eta^2 D_{44}^a + A_{44}^{aa} + A_{45}^{ad} \; ; \quad XR_{T99}^a = A_{45}^a - 4\eta^2 D_{45}^a + A_{44}^{ac} + A_{45}^{ab}$$

$$XR_{T88}^d = A_{45}^d - 4\eta^2 D_{45}^d + A_{45}^{ad} + A_{55}^{dd} \; ; \quad XR_{T99}^d = A_{55}^d - 4\eta^2 D_{55}^d + A_{45}^{cd} + A_{55}^{bd}$$

$$XR_{P1} = E_{11,11} + E_{16,12} \; ; \quad XR_{P2} = E_{16,11} + E_{12,12}$$

$$XR_{P3} = F_{11,111} + 2F_{16,112} + F_{12,122} \; ; \quad XR_{P4} = R_{18X,11} + R_{19X,12}$$

$$XR_{P5} = R_{20X,11} + R_{21X,12}$$

$$R_{18X} = F_{11} + F_{11}^a + F_{16}^d - \tfrac{4}{3}\eta^2 H_{11} \; ; \quad R_{19X} = F_{16} + F_{16}^a + F_{12}^d - \tfrac{4}{3}\eta^2 H_{16}$$

$$R_{20X} = F_{16} + F_{16}^b + F_{11}^c - \tfrac{4}{3}\eta^2 H_{16} \; ; \quad R_{21X} = F_{12} + F_{12}^b + F_{16}^c - \tfrac{4}{3}\eta^2 H_{12}$$

$$XR_{P6} = E_{16,12} + E_{66,22} \; ; \quad XR_{P7} = E_{66,12} + E_{26,22}$$

$$XR_{P8} = F_{16,112} + 2F_{66,122} + F_{26,222} \; ; \quad XR_{P9} = R_{22X,12} + R_{23X,22}$$

$$XR_{P10} = R_{24X,12} + R_{25X,22}$$

$$R_{22X} = F_{16} + F_{16}^a + F_{66}^d - \tfrac{4}{3}\eta^2 H_{16} \; ; \quad R_{23X} = F_{66} + F_{66}^a + F_{26}^d - \tfrac{4}{3}\eta^2 H_{66}$$

$$R_{24X} = F_{66} + F_{66}^b + F_{16}^c - \tfrac{4}{3}\eta^2 H_{66} \; ; \quad R_{25X} = F_{26} + F_{26}^b + F_{66}^c - \tfrac{4}{3}\eta^2 H_{26}$$

$$XR_{RR1X} = D_{44} + D_{44}^a + D_{45}^d - 4\eta^2 F_{44} \; ; \quad XR_{RR2X} = D_{45} + D_{44}^c + D_{45}^b - 4\eta^2 F_{45}$$

$$XR_{26X2} = \mathscr{D}_{11}^{a}2_{,11} + \mathscr{D}_{16}^{a}2_{,12} \; ; \quad XR_{27X2} = \mathscr{D}_{16}^{a}2_{,11} + \mathscr{D}_{12}^{a}2_{,12}$$

$$XR_{28X2} = \mathscr{E}_{11}^{a}2_{,111} + 2\mathscr{E}_{16}^{a}2_{,112} \, \mathscr{E}_{12}^{a}2_{,122}$$

$$XR_{29X2} = R2_{R1X,11} + R2_{R2X,12} \; ; \quad XR_{30X2} = R2_{R3X,11} + R2_{R4X,12}$$

$$R2_{R1X} = \mathscr{D}_{11}^{aa}2 + \mathscr{D}_{16}^{ad}2 + \mathscr{E}_{11}^{a}2 + \mathscr{E}_{11}^{a}2 + \mathscr{E}_{16}^{ad}2 + \mathscr{F}_{11}^{a}2 + \mathscr{F}_{11}^{aa}2 + \mathscr{F}_{16}^{ad}2$$

$$R2_{R2X} = \mathscr{D}_{12}^{ad}2 + \mathscr{D}_{16}^{aa}2 + \mathscr{E}_{12}^{ad}2 + \mathscr{E}_{16}^{a}2 + \mathscr{E}_{16}^{aa}2 + \mathscr{F}_{12}^{ad}2 + \mathscr{F}_{16}^{a}2 + \mathscr{F}_{16}^{aa}2$$

$$R2_{R3X} = \mathscr{D}_{11}^{ac}2 + \mathscr{D}_{16}^{ab}2 + \mathscr{E}_{12}^{ac}2 + \mathscr{E}_{16}^{a}2 + \mathscr{E}_{16}^{ab}2 + \mathscr{F}_{16}^{a}2 + \mathscr{F}_{11}^{ac}2 + \mathscr{F}_{16}^{ab}2$$

$$R2_{R4X} = \mathscr{D}_{12}^{ab}2 + \mathscr{D}_{16}^{ac}2 + \mathscr{E}_{12}^{ab}2 + \mathscr{E}_{16}^{ac}2 + \mathscr{F}_{12}^{a}2 + \mathscr{F}_{16}^{ac}2$$

$$XR_{31X2} = \mathscr{D}_{12}^{d}2_{,12} + \mathscr{D}_{26}^{d}2_{,22} \; ; \quad XR_{32X2} = \mathscr{D}_{26}^{d}2_{,12} + \mathscr{D}_{22}^{d}2_{,22}$$

$$XR_{33X2} = \mathscr{E}_{12}^{d}2_{,112} + 2\mathscr{E}_{26}^{d}2_{,122} + \mathscr{E}_{22}^{d}2_{,222}$$

$$XR_{34X2} = R2_{R5X,12} + R2_{R6X,22} \; ; \quad XR_{35X2} = R2_{R7X,12} + R2_{R8X,22}$$

$$R2_{R5X} = \mathscr{D}_{12}^{ad}2 + \mathscr{D}_{26}^{dd}2 + \mathscr{E}_{12}^{d}2 + \mathscr{E}_{12}^{ad}2 + \mathscr{E}_{26}^{dd}2 + \mathscr{F}_{21}^{d}2 + \mathscr{F}_{21}^{ad}2 + \mathscr{F}_{26}^{dd}2$$

$$R2_{R6X} = \mathscr{D}_{22}^{dd}2 + \mathscr{D}_{26}^{ad}2 + \mathscr{E}_{22}^{dd}2 + \mathscr{E}_{26}^{d}2 + \mathscr{E}_{26}^{ad}2 + \mathscr{F}_{22}^{dd}2 + \mathscr{F}_{26}^{d}2 + \mathscr{F}_{26}^{ad}2$$

$$R2_{R7X} = \mathscr{D}_{21}^{cd}2 + \mathscr{D}_{26}^{bd}2 + \mathscr{E}_{12}^{cd}2 + \mathscr{E}_{26}^{d}2 + \mathscr{E}_{26}^{bd}2 + \mathscr{F}_{26}^{d}2 + \mathscr{F}_{12}^{cd}2 + \mathscr{F}_{26}^{bd}2$$

$$R2_{R8X} = \mathscr{D}_{22}^{bd}2 + \mathscr{D}_{26}^{cd}2 + \mathscr{E}_{22}^{bd}2 + \mathscr{E}_{26}^{cd}2 + \mathscr{F}_{22}^{d}2 + \mathscr{F}_{26}^{cd}2$$

$$XR_{36X2} = \mathscr{D}_{16}^{a}2_{,12} + \mathscr{D}_{66}^{a}2_{,22} \; ; \quad XR_{37X2} = \mathscr{D}_{66}^{a}2_{,12} + \mathscr{D}_{26}^{a}2_{,22}$$

$$XR_{38X2} = \mathscr{E}_{16}^{a}2_{,112} + 2\mathscr{E}_{66}^{a}2_{,122} + \mathscr{E}_{26}^{a}2_{,222}$$

$$XR_{39X2} = R2_{R10X,12} + R2_{R11X,22} \; ; \quad XR_{40X2} = R2_{R12X,12} + R2_{R13X,22}$$

$$R2_{R10X} = \mathscr{D}_{16}^{aa}2 + \mathscr{D}_{66}^{ad}2 + \mathscr{E}_{26}^{a}2 + \mathscr{E}_{16}^{aa}2 + \mathscr{E}_{66}^{ad}2 + \mathscr{F}_{16}^{a}2 + \mathscr{F}_{16}^{aa}2 + \mathscr{F}_{66}^{ad}2$$

$$R2_{R11X} = \mathscr{D}_{26}^{ad}2 + \mathscr{D}_{66}^{aa}2 + \mathscr{E}_{26}^{ad}2 + \mathscr{E}_{66}^{a}2 + \mathscr{E}_{66}^{aa}2 + \mathscr{F}_{26}^{ad}2 + \mathscr{F}_{66}^{a}2 + \mathscr{F}_{66}^{aa}2$$

$$R2_{R12X} = \mathscr{D}_{16}^{ac}2 + \mathscr{D}_{66}^{ab}2 + \mathscr{E}_{16}^{ac}2 + \mathscr{E}_{66}^{a}2 + \mathscr{E}_{66}^{ab}2 + \mathscr{F}_{66}^{a}2 + \mathscr{F}_{16}^{ac}2 + \mathscr{F}_{66}^{ab}2$$

$$R2_{R13X} = \mathscr{D}_{26}^{ab}2 + \mathscr{D}_{66}^{ac}2 + \mathscr{E}_{26}^{ab}2 + \mathscr{E}_{66}^{ac}2 + \mathscr{F}_{26}^{a}2 + \mathscr{F}_{66}^{ac}2$$

$$XR_{41X2} = \mathscr{D}_{16}^{d}2_{,11} + \mathscr{D}_{66}^{d}2_{,12} \; ; \quad XR_{42X2} = \mathscr{D}_{66}^{d}2_{,11} + \mathscr{D}_{26}^{d}2_{,12}$$

$$XR_{43X2} = \mathscr{E}_{16}^{d}2_{,111} + 2\mathscr{E}_{66}^{d}2_{,112} + \mathscr{E}_{26}^{d}2_{,222}$$

$$XR_{44X2} = R2_{R14X,11} + R2_{R15X,12} \; ; \quad XR_{45X} = R2_{R16,11X} + R2_{R17X,12}$$

$$R2_{R14X} = \mathscr{D}_{16}^{ad}2 + \mathscr{D}_{66}^{dd}2 + \mathscr{E}_{16}^{d}2 + \mathscr{E}_{16}^{ad}2 + \mathscr{E}_{66}^{dd}2 + \mathscr{F}_{16}^{d}2 + \mathscr{F}_{16}^{ad}2 + \mathscr{F}_{66}^{dd}2$$

$$R2_{R15X} = \mathscr{D}_{26}^{dd}2 + \mathscr{D}_{66}^{ad}2 + \mathscr{E}_{26}^{dd}2 + \mathscr{E}_{66}^{d}2 + \mathscr{E}_{66}^{ad}2 + \mathscr{F}_{26}^{dd}2 + \mathscr{F}_{66}^{d}2 + \mathscr{F}_{66}^{ad}2$$

$$R2_{R16X} = \mathscr{D}_{16}^{cd}2 + \mathscr{D}_{66}^{bd}2 + \mathscr{E}_{16}^{cd}2 + \mathscr{E}_{66}^{d}2 + \mathscr{E}_{66}^{bd}2 + \mathscr{F}_{66}^{d}2 + \mathscr{F}_{16}^{cd}2 + \mathscr{F}_{66}^{bd}2$$

$$R2_{R17X} = \mathscr{D}_{26}^{bd}2 + \mathscr{D}_{66}^{cd}2 + \mathscr{E}_{26}^{bd}2 + \mathscr{E}_{66}^{cd}2 + \mathscr{F}_{26}^{d}2 + \mathscr{F}_{66}^{cd}2$$

$$XR_{46X2} = \mathscr{B}_{44}^{a}2 + \mathscr{B}_{44}^{aa}2 + \mathscr{B}_{45}^{ad}2 + \mathscr{D}_{44}^{aa}2 + \mathscr{D}_{45}^{ad}2 + \mathscr{E}_{44}^{a}2 + \mathscr{F}_{44}^{aa}2 + \mathscr{F}_{45}^{ad}2$$

$$XR_{47X2} = \mathscr{B}_{45}^{a}2 + \mathscr{B}_{44}^{ac}2 + \mathscr{B}_{45}^{ab}2 + \mathscr{D}_{44}^{ac}2 + \mathscr{D}_{45}^{ab}2 + \mathscr{E}_{45}^{a}2 + \mathscr{F}_{44}^{ac}2 + \mathscr{F}_{45}^{ab}2$$

$$XR_{48X2} = \mathscr{B}_{45}^{d}2 + \mathscr{B}_{45}^{ad}2 + \mathscr{B}_{55}^{dd}2 + \mathscr{D}_{45}^{ad}2 + \mathscr{D}_{55}^{dd}2 + \mathscr{E}_{45}^{d}2 + \mathscr{F}_{45}^{ad}2 + \mathscr{F}_{55}^{dd}2$$

$$XR_{49X2} = \mathscr{B}_{55}^{d}2 + \mathscr{B}_{45}^{cd}2 + \mathscr{B}_{55}^{bd}2 + \mathscr{D}_{45}^{cd}2 + \mathscr{D}_{55}^{bd}2 + \mathscr{E}_{55}^{d}2 + \mathscr{F}_{45}^{cd}2 + \mathscr{F}_{55}^{bd}2$$

The quantities for the shear energy contribution in the plane (y, z) are not reported, since they are similar to those for the plane (x, z), replacing x with y.

References

[Bert 1984] C. W. Bert, "A critical review of new plate theories applied to laminated composites", *Compos. Struct.* **2** (1984), 329–347.

[Bolotin 1996] V. V. Bolotin, "Delaminations in composite structures: its origin, buckling, growth and stability", *Compos. B: Eng.* **27** (1996), 129–145.

[Carvalho and Guedes Soares 1996] A. Carvalho and C. Guedes Soares, "Dynamic response of rectangular plates of composite materials subjected to impact loads", *Compos. Struct.* **34** (1996), 55–63.

[Chai and Gädke 1999] Y. Chai and M. Gädke, "Impact damage simulation and compression after impact of composite stiffened panels", Dlr report 1b 20, DLR — German Aerospace Center, Institute of Structural Mechanics,, 1999. 131–199.

[Choi 2006] I. H. Choi, "Contact force history analysis of composite sandwich plates subjected to low-velocity impact", *Compos. Struct.* **75** (2006), 582–586.

[Choi and Chang 1992] H. Y. Choi and F. K. Chang, "A model for predicting damage in graphite/epoxy laminated composites resulting from low-velocity point impact", *J. Compos. Mater.* **26** (1992), 2134–2169.

[Cox 1999] B. N. Cox, "Constitutive model for a fiber tow bridging a delamination crack", *Mech. Adv. Mater. Struct.* **6**:2 (1999), 117–151.

[Crook 1952] A. W. Crook, "A study of some impacts between metal bodies by a piezoelectric method", pp. 377–380 in *Proceeding of the Royal Society Series A*, vol. 212, London, 1952.

[Davies and Olsson 2004] G. A. Davies and R. Olsson, "Impact on composite structures", *The Aeronautical Journal* **11** (2004), 541–564.

[Echaabi and Trochu 1996] J. F. Echaabi and F. Trochu, "Review of failure criteria of fibrous composite materials", *Polym. Compos.* **17** (1996), 786–798.

[Ferrero and Icardi 2006] L. Ferrero and U. Icardi, "Improving energy absorption and dissipation of composites through optimized tailoring", in *Proceedings of the International Mechanical Engineering Congress and Exposition, IMECE*, IMECE2006-13329, ASME, Chicago, IL, 2006.

[Ferrero and Icardi 2007] L. Ferrero and U. Icardi, "Optimization of multi-core sandwich composites undergoing impact loads", in *Proceeding of the International Mechanical Engineering Congress and Exposition, IMECE*, IMECE2007-42851, ASME, Seattle, WA, 2007.

[Fuchiyama and Noda 1995] T. Fuchiyama and N. Noda, "Analysis of thernal stress in a plate of functionally gradient material", *JSAE Rev.* **6** (1995), 263–268.

[Georgi 1979] H. Georgi, "Dynamic damping investigations on composites", pp. 9.1–9.20 in *Proceeding of the 48th Meeting AGARD*, Williamsbourg, 1979.

[Goldberg 2001] K. R. Goldberg, "Implementation of fiber substructuring into strain rate dependent micromechanics analysis of polymer matrix composites", Technical report NASA/TM-2001-210822, NASA, 2001.

[Hoa and Feng 1998] S. V. Hoa and W. Feng, *Hybrid finite element method for stress analysis of laminated composites*, Kluwer Academic Publications, Boston, 1998.

[Hou et al. 2000] J. P. Hou, N. Petrinic, C. Ruiz, and S. R. Hallet, "Prediction of impact damage in composite plates", *Compos. Sci. Technol.* **60** (2000), 273–281.

[Hou et al. 2001] J. P. Hou, N. Petrinic, and C. Ruiz, "A delamination criterion for laminated composites under low velocity impact", *Compos. Sci. Technol.* **61** (2001), 2069–2074.

[Icardi 1998] U. Icardi, "Eight-noded zig-zag element for deflection and stress analysis of plates with general lay-up", *Compos. B: Eng.* **29** (1998), 435–41.

[Icardi 2001] U. Icardi, "Higher-order zig-zag model for analysis of thick composite beams with inclusion of transverse normal stress and sublaminates approximations", *Compos. B: Eng.* **32** (2001), 343–354.

[Icardi 2005] U. Icardi, "C^o plate element for global/local analysis of multilayered composites, based on a 3D zig-zag model and strain energy updating", *Int. J. Mech. Sci.* **47** (2005), 1561–1594.

[Icardi 2007] U. Icardi, "C^o plate element based on strain energy updating and spline interpolation, for analysis of impact damage in laminated composites", *Int. J. Impact Eng.* **34**:11 (2007), 1835–1868.

[Icardi and Atzori 2004] U. Icardi and A. Atzori, "Simple, efficient mixed solid element for accurate analysis of local effects in laminated and sandwich composites", *Adv. Eng. Softw.* **32**:12 (2004), 843–859.

[Icardi and Ferrero 2005] U. Icardi and L. Ferrero, "A study of energy absorption in fiber-reinforced composites: transfer form bending to shear", in *Proceedings of the 3rd International Conference on Structural Stability and Dynamics, ICSSD05*, Orlando, FL, 2005.

[Icardi and Ferrero 2006a] U. Icardi and L. Ferrero, "Impact and blast pulse: improving energy absorption of fibre-reinforced composites through optimized tailoring", in *Proceedings of the Engineering Systems and Design Analysis Conference, ESDA, ESDA2006-95772*, ASME, Torino, Italy, 2006.

[Icardi and Ferrero 2006b] U. Icardi and L. Ferrero, "Optimization of energy absorption and dissipation of composites", in *International E-conference Of Computer Science 2006*, edited by T. Simos, Lectures Series on Computer and Computational Sciences, Brill, 2006.

[Icardi and Ferrero 2006c] U. Icardi and L. Ferrero, "Optimized tailoring reducing interlaminar stresses accumulation in fiber-reinforced composites", in *Proceeding of the 2nd International Congress on Computational Mechanics and Simulation, ICCMS-06*, Guwahati, India, 2006.

[Icardi and Ferrero 2007a] U. Icardi and L. Ferrero, "Modeling assessment and optimization of impacted multi-core sandwich composites", in *Proceeding of the Society for Advancement of Material and Process Engineering Conference, SAMPE*, Baltimore, MD, 2007.

[Icardi and Ferrero 2007b] U. Icardi and L. Ferrero, "Modeling techniques assessment and optimization of laminated and sandwich composites undergoing impact loads", in *Proceeding of the 12th Aerospace and Sciences and Aviation Technology, ASAT*, 144, Cairo, Egypt, 2007.

[Icardi and Zardo 2005] U. Icardi and G. Zardo, "C^o plate element for delmination damage analysis, based on a zig-zag model and strain energy updating", *Int. J. Impact Eng.* **31** (2005), 579–606.

[Icardi et al. 2007] U. Icardi, S. Locatto, and A. Longo, "Assessment of recent theories for predicting failure of composite laminates", *Appl. Mech. Rev.* **60**:2 (2007), 76–86.

[Jones 1999] R. M. Jones, *Mechanics of composite maerials*, Taylor and Francis, Philadelfia, 1999.

[Joshi and Sun 1987] S. P. Joshi and C. T. Sun, "Impact-indiced fracture initiation and detailed dynamic stress field in the vicinity of impact", pp. 177–185 in *Proceeding of the 2nd American Society of Composites Technical Conference*, Newmark, DE, 1987.

[Jung 2001] W. Y. Jung, "A combined honeycomb and solid viscoelastic material for structural damping applications", pp. 41–43 in *Thrust area 2: seismic retrofit of acute care facilities*, Department of Civil, Structural & Environmental Engineering, University at Buffalo, 2001.

[Lakes 2002] R. S. Lakes, "High damping composite materials: effect of structural hierarchy", *J. Compos. Mater.* **36**:3 (2002), 287–297.

[Lee et al. 1997] Y. S. Lee, K. H. Kang, and O. Park, "Response of Hybrid laminated Composite Plates under loa-velocity Impact", *Comput. Struct.* **65**:6 (1997), 965–974.

[Librescu and Reddy 1986] L. Librescu and J. N. Reddy, "A critical review and generalization of transverse shear deformable anisotropic plate theories", pp. 32–43 in *Euromech Colloqioum 219, Refined dynamical theories of beams, plates and shells and their applications, Kassel*, edited by I. Elishakoff and H. Irretier, Springer Verlag, Heidelberg, September 23–26 1986.

[Liou 1997] W. J. Liou, "Contact laws of carbon/epoxy laminated composite plate", *J. Reinf. Plast. Compos.* **16**:2 (1997), 155–166.

[Loubignac et al. 1978] C. Loubignac, C. Cantin, and C. Touzot, "Continuous stress fields in finite element analysis", *AIAA J.* **15** (1978), 1645–1647.

[Matemilola and Stronge 1995] S. A. Matemilola and W. J. Stronge, "Impact induced dynamic deformations and stresses in CFRP composite laminates", *Compos. Eng.* **5**:2 (1995), 211–222.

[McCoucheon 2004] D. M. McCoucheon, "Machine augmented composite materials for damping purposes", Degree of master of science thesis, Texas A&M University, 2004.

[Nahas 1986] M. N. Nahas, "Survey of failure and post-failure theories of laminated fibre reinforced composites", *J. Compos. Tech. Res.* **8** (1986), 138–153.

[Nakazawa 1984] S. Nakazawa, *Mixed finite elements and iterative solution procedures*, Iterative Methods in Non-Linear Problems, Pineridge, 1984.

[Noor and Burton 1989] A. K. Noor and W. S. Burton, "Assessment of shear deformation theories for multilayered composite plates", *Appl. Mech. Rev.* **42** (1989), 1–13.

[Noor and Burton 1990] A. K. Noor and W. S. Burton, "Assessment of computational models for multilayered composite shells", *Appl. Mech. Rev.* **43** (1990), 67–97.

[Noor and Burton 1992] A. K. Noor and W. S. Burton, "Computational models for high-temperature multilayered composite plates and shells", *Appl. Mech. Rev.* **45** (1992), 419–444.

[Noor et al. 1996] A. K. Noor, W. S. Burton, and C. W. Bert, "Computational models for sandwich panels and shells", *Appl. Mech. Rev.* **49** (1996), 155–199.

[Paris 2001] F. Paris, "A study of failure criteria of fibrous composite materials", Technical report NASA/CR-2001-210661, NASA, 2001.

[Pedersen 2003] P. Pedersen, "A note on design of fiber-nets for maximum stiffness", *J. Elasticity* **73**:1–3 (2003), 127–145.

[Reddy 1982] J. N. Reddy, "Survey of recent research in the analysis of composite plates", *Compos. Technol. Rev.* **4** (1982), 101–104.

[Reddy 1990] J. N. Reddy, "A review of refined theories of laminated composite plates", *Shock Vibr. Dig.* **22** (1990), 3–17.

[Reddy 2003] J. N. Reddy, *Mechanics of laminated composite plates and shells: Theory and analysis*, 2nd Edition ed., CRC Press, Boca Raton, FL, 2003.

[Reddy and Robbins 1994] J. N. Reddy and D. H. J. Robbins, "Theories and computational models for composite laminates", *Appl. Mech. Rev.* **47** (1994), 147–169.

[Rowlands 1985] R. E. Rowlands, "Strength (failure) theories and their experimental correlations", pp. 71–125 in *Handbook of Composites*, vol. 3, Elsevier Science Publ., 1985.

[Setoodeh et al. 2005] S. Setoodeh, M. M. Abdalla, Z. Gurdal, and B. Tatting, "Design of variable-stiffness composite laminates for maximum in-plane stiffness using lamination parameters", pp. 3473–3481 in *Proceeding of the 46th AIAA/ASME/ASCE/ AHS/ASC Struc., Struct. Dynam and Appl. Conf., 13th AIAA/ ASME/ AHS Adap. Struc. Conf., 7th AIAA Non-Determ Appr. Forum*, 2005.

[Suzuky et al. 2003] K. Suzuky, K. Kageyama, I. Kimpara, and S. Hotta, "Vibration and damping prediction of laminates with constrained viscoelastic layers", *Mech. Adv. Mater. Struct.* **10**:2 (2003), 43–73.

[Tan and Sun 1985] T. M. Tan and C. T. Sun, "Use of statical indentation laws in the impact analysis of laminated composite plates", *J. Appl. Mech. (Trans. ASME)* **52** (1985), 6–12.

[Tennyson and Wharam 1985] R. C. Tennyson and G. E. Wharam, "Evaluation of failure criterion for graphite-epoxy", Technical report NASA CR-172547, NASA, 1985.

[Wu and Shyu 1993] E. Wu and K. Shyu, "Response of composite laminates of contact loads and relationship to low-velocity impact", *J. Compos. Mater.* **27**:15 (1993), 1443–1464.

[Yigit and Christoforou 1995] A. S. Yigit and A. P. Christoforou, "Impact dynamics of composite beams", *Compos. Struct.* **32** (1995), 187–195.

[Zienkiewicz and Taylor 1994] O. C. Zienkiewicz and R. L. Taylor, *The finite element method*, vol. 1, 4th Ed. ed., McGraw-Hill, London, UK, 1994.

[Zinoviev and Ermakov 1994] P. A. Zinoviev and Y. N. Ermakov, *Energy dissipation in composite materials*, Technomic Pub. Co., Lancaster, UK, 1994.

UGO ICARDI: ugo.icardi@polito.it
DIASP, Politecnico di Torino, Corso Duca degli Abruzzi 24, 10129 Torino, Italy

LAURA FERRERO: laura.ferrero@polito.it
DIASP, Politecnico di Torino, Corso Duca degli Abruzzi 24, 10129 Torino, Italy